Computer Networks 177 (2020) 107280

Contents lists available at ScienceDirect

Computer Networks

journal homepage: www.elsevier.com/locate/comnet

Review article

Analysis of hidden node problem in LTE networks deployed in unlicensed spectrum

Pablo Campos*, Ángela Hernández-Solana, Antonio Valdovinos-Bardají

Aragon Institute for Engineering Research (I3A), University of Zaragoza, Zaragoza, 50018, Spain

ARTICLE INFO

Keywords:
LAA
LBT
CQI
RSRQ
Hidden node problem

ABSTRACT

LTE operation in the unlicensed spectrum based on Licensed-Assisted Access (LAA) is being considered as an option to increase the capacity of 4G/5G wireless networks. This solution allows the eNodeB to contend with other nodes by accessing the shared medium and, through carrier aggregation (CA), to use both licensed and unlicensed bands to deliver best effort services. Nevertheless, the hidden node problem over shared medium access networks is an obstacle that must be addressed in order to reduce or avoid performance degradation problems. The metrics associated to LAA reflect the behavior of a node facing collisions. A better understanding of these metrics can help to identify nodes affected by hidden terminals, making it possible to take smart decisions about the continuity of a node on the unlicensed band, resulting in an improved network performance. In this paper, we first study the Channel Quality Indicator (CQI), Reference Signal Received Power (RSRP) and Reference Signal Received Quality (RSRQ) metrics on the context of LAA for a User Equipment (UE) that is facing different levels of interference. Then, a combination of the above metrics is used in order to develop an algorithm for collision detection. Finally, the performance of the algorithm is evaluated using a simulation tool under realistic channel conditions. The results show that is feasible to detect, with an adequate accuracy level, if a node is affected by collisions and subsequently if this node is located in hidden area. This is demonstrated with different levels of interference, realistic channel conditions and users in movement inside the hidden area.

1. Introduction

The continuous increase in traffic and mobile devices during the past decade [1], along with the higher rates of the air interface that the Third Generation Partnership Project (3GPP) finds out with the standardization of Fifth Generation (5G), promises a series of challenges and opportunities to network operators that, if addressed correctly, will improve the network performance. With this in mind, 3GPP has considered to enter in the competition of unlicensed bands with the use of Licensed-Assisted Access (LAA) to boost LTE (Long Term Evolution) coverage and capacity using small cells in both licensed and unlicensed bands in a cost-efficient manner. Here, the licensed channel remains the primary carrier, delivering control and signaling, and the unlicensed band can be used for best effort service upon availability [2]. Also, because of the wide range of unlicensed bands, LAA can be seen as viable candidate for 4G/5G services, where using common designs across licensed and unlicensed bands can provide efficiency and flexibility in resource management, and simplicity in implementation. LAA is a standardized version of LTE in unlicensed band introduced in 3GPP Release 13, which employs a Listen Before Talk (LBT) algorithm to access the medium [3], thus allowing a “fair” and “friendly” coexistence with other carrier sense technologies that are currently operating over the ISM (Industrial, Scientific and Medical) band, mainly 2.4 GHz and 5.1 GHz.

It is expected that typical scenarios for 4G/5G in unlicensed spectrum will have many similarities with current Wi-Fi networks, namely short range coverage, hostile environments and low mobility. When LAA from different LTE operator networks or other existing technologies like Wi-Fi nodes enter in action over a shared geographical area, there is a high probability that common overlapped areas will emerge reusing the same channel frequency. It is true that, to ensure coexistence and to minimize interference, LAA-LTE eNBs try to select a channel that is not used by nearby Wi-Fi nodes, or other LAA eNBs by using a channel selection mechanism.

Nevertheless, since classical LTE-based radio deployments are expected to reach saturation, especially in high-density areas, extensive use of LAA-LTE is anticipated, which will result in an increased spectrum reuse in unlicensed band. For instance, the deployment of high amount of sensors, predicted in 5G networks, will require probably the use of unlicensed bands in scenarios with high traffic loads, where the limited licensed band cannot afford the demand of the service. The massive use of free bands for different operators, together with other technologies that will make use of the band, will trigger an increased level

* Corresponding author.
E-mail addresses: pcampos@unizar.es (P. Campos), anhersol@unizar.es (Á. Hernández-Solana), toni@unizar.es (A. Valdovinos-Bardají).

https://doi.org/10.1016/j.comnet.2020.107280
Received 12 January 2020; Received in revised form 19 March 2020; Accepted 21 April 2020
Available online 13 May 2020

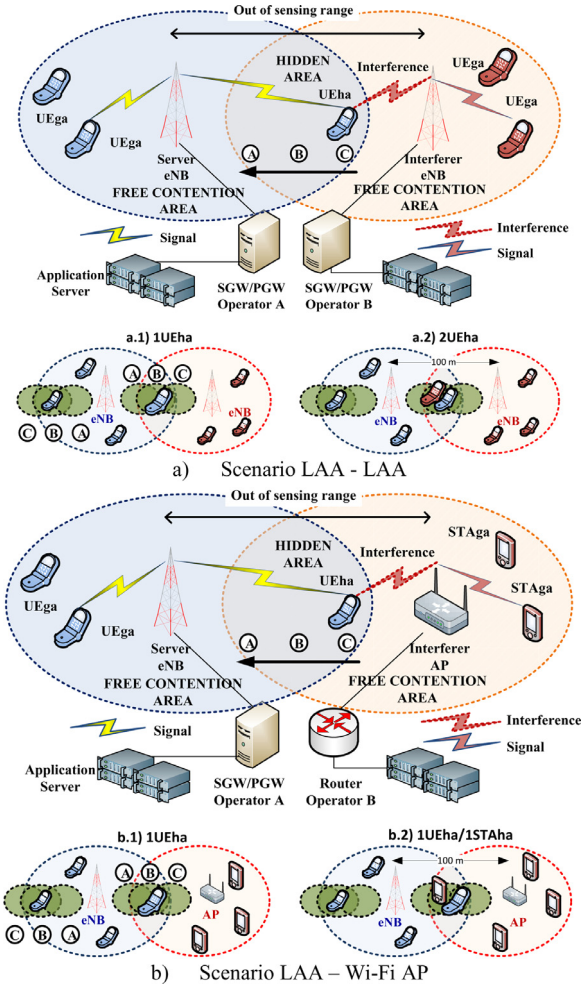

Fig. 1. Hidden node condition.

of interference coming from hidden nodes, which cannot be avoided by LBT algorithm. Stopping the waste of radio resources by UEs severely affected by interference may lead to an increase in the channel capacity. Besides, when working in unlicensed bands may occur that sensors that at the beginning are located on a free contention area, later may be affected by a hidden node that belongs to another operator. Early detection of this problem permits the optimization of the capabilities of the system by the LTE operator.

LTE based systems are more robust regarding to intra-operator interference than Wi-Fi due to their inherent centralized radio resource management strategies, but coexistence between eNBs deployed by different LAA operators, as well as coexistence between LAA and Wi-Fi, should be carefully investigated.

Thus, in order to ensure coexistence and to minimize interference in these heterogeneous networks, a deep understanding of the real effect that nodes located in hidden areas have over LAA networks is necessary. The present contribution focuses mainly on the coexistence of LAA networks from different operators, and also on the coexistence of LAA with other Carrier Sense Multiple Access-Collision Avoidance (CSMA/CA) technologies such as Wi-Fi. It investigates a set of metrics inherent to LTE technology that permit the detection of high-interfered nodes located in common overlapped areas that we define as *hidden areas*.

The hidden node problem is a classic issue in carrier sense access technologies. Fig. 1 illustrates this problem: two base stations, a LAA evolved Node B (eNB) and another eNB belonging to different operators or a Wi-Fi Access Point (AP) are out of sensing range (e.g. due to fading, propagation losses, obstruction, etc.) so they are not able to detect the presence of each other. In this scenario, both base stations may transmit simultaneously and they will not be able to detect the generated collision, thus both nodes continue transmitting, even when they have their collision detection algorithms working permanently. When this happens, the UE located in the hidden area receives a high and constant interference while it is receiving data.

However, not only a high level of interference is expected on LTE UEs from Wi-Fi stations (STAs) located over hidden areas when collisions occur but also a large fluctuation of the Signal to Interference and Noise Ratio (SINR) due to alternation between collisions and no collisions. In LTE, these effects lead to an increasing and variable use of radio resources. Under this condition, an efficient scheduling is not feasible and inter-cell interference coordination/mitigation is not possible.

As seen in Fig. 1, it is common that the free contention area covers a surface larger than the hidden area, making it possible to apply channel reuse techniques for most of the UEs near the eNB. However, as long as the eNB tries to satisfy the service requirements of all UEs, the waste of resources associated to UEs affected by the hidden problem, noted as (UEha), may spoil the overall service. This is mainly due to nodes in hidden areas require continuous retransmissions or the use of an excessive number of physical resource blocks (RB), defined in Table 6.2.3-1 in [4], with lower MCS (Modulation and Coding Scheme). As a result, they steal resources to UEs located on non-contending areas, noted as (UEga), and may even affect their performance.

Even though Quality of Service (QoS) in an unlicensed band cannot be assured because of the lack of guaranteed access to the channel, the detection of UEs affected by hidden nodes is necessary in order to avoid the misuse of radio resources that certainly affects dramatically the limited QoS offered in these technologies.

Unlike other CSMA/CA technologies, which through the interchange of Ready-To-Send Clear-To-Send (RTS/CTS) signals try to avoid the hidden node problem, LAA does not have a mechanism to detect the presence of hidden nodes. Thus, the aim of this paper is to analyze the potential use of physical measurements reported by UEs to develop an algorithm that allows the detection of UEs in hidden areas. Specifically, we study the UE reported parameters such as Reference Signal Received Power (RSRP), Reference Signal Received Quality (RSRQ), together with Channel Quality Indicator (CQI), to establish how bad channel conditions and/or interference affect each of these metrics. These parameters are obtained for both the licensed and unlicensed bands, but for hidden node detection we use the measurements coming from the unlicensed band. After this analysis, we use a combination of some of these metrics to implement a solution that makes feasible the detection of hidden nodes with a good level of accuracy.

The next conditions should be accomplished by the planned solution:

- It should use the metrics already existing in LTE, not making changes to the current standard.
- The considered scenarios should be similar to the ones that Wi-Fi or Ad-hoc technologies are nowadays working on, where short coverture, low mobility and hostile environment are a premise.
- The solution should work limiting the signaling overhead between UE and eNB. In addition, coordination between nodes of different operators should not be required.
- Finally, the solution should be independent of the technology of the interferer node. This implies that it should work no matter if the source of interference is another LAA, Wi-Fi or another technology working in the same band.

All these aspects have been considered in the design of our algorithm, which permits the detection of UEs facing interference caused by the hidden node problem. This information is useful when deciding whether a terminal should be served in the unlicensed band, or transferred to the licensed spectrum.

1.1. Contributions

In this paper, we discuss the MAC-level problems in the DL (downlink) part of the spectrum. UL (uplink) is out of the scope of the paper. Considering all the aspects detailed before, the main contributions in this paper are:

- We analyze the RSRP, RSRQ and CQI metrics reported by UEs affected by different levels of server and interferer traffic loads. The analyzed UEs are located over *hidden area* (UEha) and free contention areas, which we call UE *over good areas* (UEga). These analyses permit to identify how these metrics are affected by bad channel conditions and high interference.
- We develop an algorithm that, combining CQI, RSRP, and RSRQ measurements, makes it feasible to detect UEs affected by collisions when they are facing the hidden terminal problem.
- The detection accuracy of the algorithm is evaluated quantitatively through the use of a simulation tool.

The rest of this paper is organized as follows. First, section 2 summarizes previous related works and makes a short description about the work to be developed. Section 3 describes the system model detailing the mains aspects of the technology and features regarding to the channel, scenarios and simulation tool. In section 4, we make a detailed analysis of the metrics that could be potentially used to hidden node detection. In section 5, the proposed collision detection algorithm and its operation are introduced. Section 6 is dedicated to simulation results and discussion. Finally, the main conclusions are detailed in section 7.

2. Related work and proposed approach

The problem of hidden nodes has been studied for networks employing carrier sense medium access techniques like 802.11 and ad-hoc networks. Proactive and reactive detection constitute two methods to address this problem. In both cases, the main issues are the reliability of the detection method, the amount of signaling overhead required for making predictions and how much interference or service degradation can be maintained before proposing a reactive action.

Few works consider the hidden node problem in the context of LAA. Among them, [5] proposes channel selection and user offloading mechanisms based on average CQI (CQIav) values reported by UEs. The proposed channel selection algorithm calculates CQIav of all UEs for each unlicensed channel (the scheme stores the maximum CQI of each UE) and selects the channel with maximum CQIav, corrected by a fairness factor. Then, the paper suggests offloading the UEs more affected by interference to the licensed channel. Likewise, authors say that offloading the UEs with the lowest CQIav is inappropriate, because these UEs may be located on cell-edge and this will not guarantee any performance improvement. The chosen criterion is offloading the UE with the highest difference between the maximum stored CQI and the current CQI. The main limitation of this method is that it needs that every UE performs a CQIav measurement per each unlicensed channel. Consequently, the eNB has to operate on each unlicensed channel for some time in order to make the method feasible, which is not practical. On the other hand, this work considers that the UE with the greatest difference is the one that most degrades the network, which is not necessarily true, especially in scenarios with realistic channel conditions and hidden nodes.

3GPP RAN1 WG explores possible solutions for the hidden node problem. In [6] the authors suggest the use of channel reservation using a full-duplex radio (FDR). The proposal assumes that an UEha is aware of the timing and period that a server eNB transmits DL data on the unlicensed channel. To avoid the hidden node problem, the UEha with FDR receives data and simultaneously sends the busy tone during the whole transmission period to nearby eNBs. By detecting the busy tone, the hidden eNBs postpone any transmission until the channel becomes idle. By using FDR technology, it is assumed that UEs can receive data and send the busy tone simultaneously over the same band. This assumption is not allowed if UE operates in FDD (Frequency Division Duplexing) mode. A main drawback of this proposal is the waste of radio resources, because any neighboring eNB is not allowed to transmit during all the time the server eNB transmits, which is not efficient. Additionally, even if LTE operates in TDD (Time Division Duplexing) mode, the implementation involves the modification of the standard.

The work in [7] proposes the use of an RTS/CTS approach; this solution is similar to the previous one, with the fundamental difference that RTS/CTS signals last a short period of time, meanwhile the busy tone lasts all transmission period. The main problem with RTS/CTS is that these signals introduce considerable overhead and may unnecessarily decrease the communication efficiency, especially over densely deployed WLANs [8,9].

A power-based approach is suggested in [10]. This work proposes to boost the power transmission to UEs affected by hidden nodes, based on their Channel State Information (CSI) feedbacks. One limitation of this solution is that by boosting the power, other nodes nearby the UEha may not be able to access the channel, since they can probably sense the power exceeding the Clear Channel Assessment (CCA) threshold. Furthermore, a higher interference in the surrounding networks is introduced.

Additionally, in [11] the use of RSSI measurements is considered with the purpose of detecting hidden nodes. To enable this approach, the UE must report its RSSI to eNB, where a comparison between UE RSSI and eNB RSSI is done and if the UE RSSI is above a threshold, and eNB is below the same threshold inside the same measurement window, the UE might be in hidden area. The problem with this method is that the document does not indicate how the threshold is obtained and also it declares that the average RSSI and channel occupancy may not be sufficient for hidden node detection.

In the present paper, we employ the statistical distribution of CQI reported by UEs to determine the channel quality around the UE and to have a first approach to hidden node detection. The analysis of these results shows that CQI by itself is not good enough to estimate the presence of hidden nodes under realistic channel conditions. Consequently, more variables are added to our detection algorithm, and other parameters such as RSRQ and RSRP are considered to obtain an accurate hidden node detector. This solution does not require coordination among nodes, which is desirable under a heterogeneous network. Finally, we measure the performance of the algorithm by conducting an extensive simulation campaign using a NS3-based simulation tool where different variables such as traffic load, traffic models, Rayleigh communication channels, UE mobility, etc. have been considered in order to test the robustness of the solution.

3. Network modeling

In this paper, we focus on hidden node detection in unlicensed LTE, implemented as a technology anchored to licensed spectrum, and in particular on LAA technology. In this section, we provide a general overview of this technology, focusing on the main features that will be helpful to understand the analysis and proposals performed in the paper. In addition, scenarios of analysis are described.

3.1. LAA technology

LTE LAA is standardized as part of 3GPP Release 13, where the unlicensed spectrum is an extension of the LTE carrier aggregation protocol [12,13]. Transmission over a licensed carrier, serving as Primary Cell (PCell), is always required, while unlicensed carriers may be used as Secondary Cells (SCell), in this case only used for DL transmissions. It implies that Radio Resource Control (RRC) to handle connections, signaling for SCell activation and deactivation, broadcasting of system information, radio link monitoring (RLM), handover management and Non-Access Stratum (NAS) functionalities such as security key exchange and mobility information are only provided through the PCell. Physical

Downlink Control Channel (PDCCH) messages, including the scheduling information, reference signals (RS), and Physical Downlink Shared Channel (PDSCH), which carries user data, can be transmitted on either licensed or unlicensed spectrum, while UL transmissions are limited to the PCell. Note that, as referred above, LTE LAA is just one kind of scenario using carrier aggregation. This implies that the UEs can report the measurements of RSRP, RSRQ and CQI for every band (licensed and unlicensed). The metrics RSRP, RSRQ and CQI are calculated in the same way no matter if these measurements come from licensed or unlicensed band, but their values depend entirely on the features of the channel and the traffic load that exist over the band where measurements are performed.

To address the coexistence of LAA and other systems such as Wi-Fi in the unlicensed spectrum, LAA uses a LBT mechanism, in such a way that, before accessing the medium, the eNB has to sense it for a randomly chosen amount of time via CCA, which is also known as *backoff procedure*. Provision of guaranteed QoS in unlicensed bands is hard to achieve due to the randomness in the access to the channel. This is the reason because high-priority traffic with strict QoS requirements will be preferably served over the licensed band (both UL and DL). Unlicensed spectrum can be utilized opportunistically for best effort traffic in DL [14,15].

The main aspects that LAA technology involves are:

- Channel sensing to detect idle channel.
- Deferred time and reservation signal.
- Discovery reference signal.
- Contention window and HARQ.

We will next explain each of them separately.

3.1.1. Channel sensing to detect idle channel

LAA eNBs listen to the channel applying CCA to check the availability of the channel before transmitting on it. A channel is judged as idle when whatever signal present in the medium (if any) during an initial CCA time does not exceed an Energy Detection (ED) threshold. 3GPP recommends that the ED threshold for LAA should be -72 dBm for a 20 MHz channel.

Then, the LAA eNBs implement category 4 LBT [16], which considers random backoff with a variable Contention Window (CW) for transmissions over user data channel (PDSCH). An eNB is allowed to transmit after sensing the channel to be IDLE during an initial CCA period (Td_cca) composed by a fixed duration $Tf = 16\ \mu s$ and a number mp CCA slots (each CCA slot duration is $Tsl_cca = 9\ \mu$s). The value of mp depends on the channel access priority class, which is used to categorize the type of traffic scheduled in the unlicensed band. For instance, 1, 1, 3 and 7 for priority classes 1, 2, 3 and 4, respectively. If channel is judged as idle during Td_cca, the eNB starts transmitting a channel reservation signal, to which other contenders will backoff and abstain from accessing the channel. This is because the eNB that wins the access to the channel has to wait until the beginning of the next subframe (synchronous with PCell) to initiate its transmission on PDSCH/PDCCH.

But, if the channel is busy, an extended CCA (eCCA) is applied. Once the channel is free for a period Td_ecca, the eNB senses the channel to be idle during a number N of eCCA slots ($Tsl_ecca = Tsl_cca = 9\ \mu$s), being N a random value of a backoff counter in the range [0, CWp]. CWp is the current CW size, which ranges between CWmin and CWmax. Each time the channel is detected to be idle for a period of one eCCA slot, the backoff counter (N) is decreased by one. If the eNB detects that the channel is occupied, the backoff counter is frozen, and the eNB continues to sense the channel until it finds it to be idle for Td_ecca. Finally, when N reaches zero the eNB is allowed to start its transmission. Note that, CW size will be increased upon collisions.

3.1.2. Deferred time and reservation signal

Once the eNB has applied LBT, and if the channel is judged as idle, the eNB is allowed to transmit during a Transmission Opportunity (TxOP) time, no longer than a Maximum Channel Occupancy Time (MCOT), which depends on the priority class [17]. The MCOT is applied to avoid that one eNB can monopolize the medium.

MCOT establishes the maximum time that a LAA DL transmission burst can use the channel continuously. Then, after completing the MCOT, in order to continue its transmission, the eNB must wait a deferred time equal to 43 μs (for priority class 3). During this time, all other eNBs or another AP can content for the channel with the exception of the eNB that was using the channel last time. After completing the deferred time, the eNB that was excluded from contention can participate again and if it obtains the channel, it can continue its previous DL transmission.

As we refer above, the eNB that wins the access to the channel has to wait until the beginning of the next subframe to initiate its transmission. In this case, the eNB generates a reservation signal until the beginning of the next subframe, so other contenders get acquainted of the busy channel state. The reservation signal fulfils its role only when the power received by other eNBs is higher than the ED threshold. Otherwise, eNBs can transmit and collisions may appear.

3.1.3. Discovery reference signal

As traffic patterns fluctuate over time and space, under-utilized eNBs can be dynamically turned off to save energy and turned on when traffic conditions demand it. Regarding the unlicensed band, because its condition of secondary cell, it is not mandatory to remain in the ON state all the time, and its state basically depends on the presence or not of traffic to transmit.

The Radio Resource Management (RRM) in LTE for both licensed and unlicensed spectrums in DL are based on the channel quality measurements obtained from Reference Signals (RS). Discovery Reference Signal (DRS) were introduced in Release 12 to support cell detection, synchronization, and RRM measurements when cells are in OFF state for appreciable fractions of time. Thus, the eNB can transmit DRSs over unlicensed SCell within a Discovery Measurement Timing Configuration (DMTC) interval that has a duration of 6 ms (from subframe 0 to subframe 5 inside PDCCH) with a period of 40/80/160 ms, although, due to CCA, exact DRS transmission period is not guaranteed. According with this, UEs need wake up on these fixed periods of time to detect, measure and report measurements to the network for efficient RRM functionalities [16].

When cells are in ON state and they have data to transmit, DRSs are embedded together with data and also transmitted over the corresponding PDCCH. In absence of data, DRSs can be sent alone over PDCCH. DRSs include several signals, such as Primary Synchronization Signal (PSS), Secondary Synchronization Signal (SSS) and Cell-Specific Reference Signal (CSI-RS).

3.1.4. Contention window and HARQ

LTE uses Hybrid Automatic Repeat Request (HARQ). In this case, the used HARQ scheme is soft combining hybrid full incremental redundancy, while a maximum of 3 retransmissions are allowed. HARQ feedbacks associated to a specific subframe are received at least 4 ms after the transmission of its Transport Block (TB) from the transmitter.

However, the most relevant details concern to the unlicensed SCell, because the eNB uses the information of Negative Acknowledgements (NACK) provided by HARQ to increase the Contention Window (CW) size. In specific, the CW size at eNB is increased if more than Z percentage of HARQs corresponding to the PDSCH transmission (user data) in a reference subframe k (defined below) are determined as NACKs. The default value of the Z parameter is 80%. Otherwise, if this threshold is

not reached, the CW size is reset to the minimum CW. The reference subframe k is typically the first one of the most recent transmission burst for which some HARQ feedback is available [18].

3.2. Scenarios

Two scenarios are considered in this work in order to assess the capabilities of UEs in the context of hidden nodes under realistic channel conditions. Fig. 1 depicts the two scenarios. Fig. 1 (a) represents two LAA networks driven by two independent operators, whereas Fig. 1 (b) illustrates one LAA network together with a Wi-Fi network. Both scenarios present similar features with the exception that the technology of the interferer network in Fig. 1 (b) is Wi-Fi.

The scenarios are working in the same downlink channel at the 5 GHz unlicensed band with a bandwidth of 20 MHz. Both eNBs in Fig. 1 (a) and the eNB and the Wi-Fi AP in Fig. 1 (b) are out of the sensing range from each other, with a portion of their coverage area overlapped.

Path loss is calculated on a per-user basis, which includes distance path loss, shadowing and multipath fading. The chosen propagation model is a modified version of ITUInH indoor to ensure Non Line of Sight (NLOS) between base stations [19]. The propagation model supports NLOS and Line of Sight (LOS) patterns as a function of the distance. Shadowing is also enabled with standard deviations of σ=3 (LOS) and σ=4 (NLOS), with a correlation distance of 8m, and Rayleigh losses are defined according to 3GPP TS 36.104 Annex B.2 [20] in order to build a frequency-selective multipath fading channel [21].

Server and interferer base stations are hidden from each other and separated by 100 m. UEs, using omnidirectional antennas, move randomly at speed of 3 Km/h. A number of M-2 UEs are located randomly over each cell's coverage, and the remaining 2 UEs in the server cell become our test nodes, named as UEha and UEga. UEha is positioned on the overlapped area and UEga is located on the free contention area. At the beginning of every realization, both test nodes, will have the same distance respect to eNB in order to suffer from similar path loss conditions. These two UEs constitute our test nodes and their results will be contrasted to obtain a better understanding about how channel and collisions affect the nodes located in the cell border. Note that some realizations for Fig. 1 (a) will have 1 UEha and others will have 2 UEha, one UE for each operator. Meanwhile, for Fig. 1 (b) some realizations will have 1 UEha, and others will have 1 UEha and 1 STAha simultaneously. In this case, the same number of M-1 STAs are located randomly over AP's coverage. The number of interferers such as eNBs, STAs or APs Wi-Fi and UEs inside the hidden area are limited. However, we are not interested in obtaining absolute results of a particular scenario but in evaluating the feasibility of the proposed method in any deployment scenario. Results depend on the total interference and not on the number of sources that generate the interference. Therefore, a unique source of interference (eNB or AP) has been used to have a better control of the received interference and of the percentage of time that a UEha is interfered. The analysis has been carried out for different values of received interference power and variable traffic load in server and interferer cells, which allows us to generalize the conclusion for scenarios with multiple interferer sources.

Additionally, the test UEs will be located in three different positions: A, B and C. Position A for UEha fits a scenario with a strong signal from the server cell and low interference. Position B for UEha corresponds to a context where power from server is reduced and from interferer is increased. Finally, in position C the UEha receives a strong interference and low power from server cell. The simulations will run separately for each position to obtain data with different levels of interference and channel conditions.

The MAC scheduler and link state algorithms are based on Proportional Fair (PF) scheduling rule and CSI measurements (mapped and reported on CQI indicator), which in turn are obtained from reference signals. CQI index is obtained from current SINR measurements. SINR values and Block Error Rate (BLER) lower than 10% are used to obtain the MCS that maximizes the spectral efficiency. The MCS selection follows the standard indicated in Table 7.1.7.1-1 of [17], with a maximum modulation order of 6 to perform at 64 QAM, which together with a 2×2 MIMO spatial multiplexing, allows to reach rates up to 120 Mbps over a 20 MHz bandwidth in the downlink. Table 7.2.3-1 in [17] is used to map the spectral efficiency to CQI index. All UEs calculate their CQIs (CQIs are a kind of CSI) and report them to their eNB, no matter if the data are addressed to them or not.

Concerning the PF scheduling rule, note that UEha receives the assigned resources following this scheduling policy as others UEs that are attached to the same eNB. PF tries to provide a similar service in the medium term to all UEs.

The UEs that are located in the hidden area and are affected by interference report lower values of CQI indexes and consequently need more radio resources to transmit the information. The additional radio resources that they need are at the expense of other UEs and this results in a lower throughput for other users (UEga). This is the reason why the identification of UEha is a key issue. When a UEha has a severe impact on throughput for the rest of UEs inside the cell, it is necessary to move it to a licensed band in order to improve the global services in the unlicensed band.

Finally, two kinds of traffic are used for the analysis. Both of them correspond to best effort. The first is FTP over UDP to simulate bursty traffic and the second is UDP with constant bit rate (CBR). Real time services had not be considered in the unlicensed band because it is not possible to guarantee a level of quality similar to the one that can be obtained using the LTE standard over licensed carriers. Service over the unlicensed band depends on the level of occupancy of the band by other LTE operators and Wi-Fi systems working in the same spectrum. FTP requests a file of 2 MB size following a Poisson distribution with an arrival rate Lambda (λ) which ranges [0.5, 3] files/second as defined in section A.2.1.3.1 in [22]. Meanwhile, UDP requests IP packets to keep a target Rate that variates [1.0, 3.5] Mbps. The files or IP packets are requested sequentially by all UEs inside of every cell. Each operator delivers their FTP or UDP traffic independently, so the server and interferer eNBs simulates different levels of traffic load for every realization.

Additionally, Wi-Fi devices (AP/STAs) share the channel with eNB transmitting in channel 36 (5.18 GHz/20 MHz bandwidth). The Wi-Fi MAC follows the carrier sense multiple access collision avoidance (CSMA/CA) protocol with periodic beacons generated by the AP. If a Wi-Fi device has data to transmit, it senses the channel. If the medium is assessed busy, the MAC defers the transmission until medium becomes idle. If the idle period is longer than the arbitration interframe space (AIFS), which is 43 μs for best effort traffic with a slot duration of 9 μs, a random backoff is performed, likewise anytime a collision occurs the backoff is increased exponentially until reaching the maximum contention window (CWmax).

During the Clear Channel Assessment, the devices sense the medium with an Energy Detection (ED) threshold set to -72 dBm to detect non Wi-Fi energy levels present on the current channel. The Preamble Detection (PD) for 802.11 frames detection is set to -82 dBm. The model performs the 802.11n standard, 2×2 MIMO with a MCS maximum of 15 using an Interval Guard of 400 ns. Table 1 summarizes the main parameters used during simulation.

Moreover, an adaptive but ideal rate control algorithm selects the best rate according to SINR of the previous packet sent. The SINR is sent back from the receiver to transmitter embedded in ACK/NACK message over an error free channel, which is the reason for "ideal". AP uses the SINR information to select the transmission rate based on a set of SINR thresholds.

4. Analysis of potential metrics suitable for hidden node detection problem

The general objective of this paper is to obtain an algorithm that permits to detect UEs that are affected by hidden nodes under a realistic

Table 1
Simulation parameters.

Parameter	Value
NS3 Version	NS-3 LBT
Inter-Site Distance (ISD)	100m
Carrier Frequency	5180 MHz DL
System Bandwidth	20MHz
Path-loss model [19]	ITU InH model
Shadowing standard deviation	σ=3 (LOS) / σ=4 (NLOS)
Shadowing correlation distance	8m
Channel/Doppler model (3Km/h)	Jakes
eNB cell parameters	
Transmission Time Interval (TTI)	1ms
RB size	12 subcarriers(RE) for 1TTI
Maximum output power eNB/UE	18 dBm/18 dBm
Antenna TX Gain eNB LBT	5dBi
Antenna TX/RX GainUE	0dBi/0dBi
Receiver noise figure eNB/UE	5dB/9dB
MIMO	2×2 Spatial Multiplexing
HARQ	IR Max. 3 reTX
Min HARQ delay	4ms
Time between CQIs	2ms
TCQI(L) updating time	200ms
RSRP/RSRQ reporting period	200ms
RLC Mode /RLC Buffer	UM RLC / 200MB
Scheduler	Proportional Fair (PF)
Access Method	LBT
ED Threshold	-72dBm
DRS Period	80ms
Delay MAC /PHY	2ms
CW Update	NACK 80%
TXOP	8ms
Wi-Fi Cell parameters	
Wi-Fi PHY standard	802.11n
Access Method	CSMA/CA
AP (TX power/Ant Gain/NF)	18dBm / 5dBi / 5dB
STA (TX power/Ant Gain/NF)	18dBm / 0dBi /9dB
ED Threshold / Preamble Detection	-72dBm / -88dBm
Traffic parameters	
UDP Packet / FTP Files	1480Bytes / 2MB
λs / λi (FTP)	[0.5, 3.0] file/s
Rs / Ri (UDP)	[1, 3.5] Mbps

channel. Nevertheless, prior to achieve this goal it is necessary to find a metric or set of metrics that can be used to design the algorithm. In our case, the analyzed metrics include:

- UEs CQI distribution, instead of mean CQI
- Physical measured reports as RSRP, RSSI and RSRQ.

4.1. CQI distribution and hidden node detection

We analyze the potential use of the statistical distribution of CQI indexes reported by the UE in order to discover if a specific terminal is affected by collisions coming from interferer eNB or Wi-Fi. Additionally, we explore the relationship between the traffic load of the interferer node with the CQI distribution of UEs located in the hidden area. The objective is to determine if CQI statistics varying with interferer traffic load will be helpful for discovering if a specific UE is affected by the hidden node problem.

The UE generates a periodic CQI which is a representative value of the channel state calculated over all RBs in use during one Transmission Time Interval (TTI) (wideband method). The reported CQI index ranges from 0 to 15 where zero represents out of range and 15 the best channel conditions. In the context of LAA, CQIs are obtained periodically every time that a DRS or user data are transmitted by the server eNB. This implies that during null periods of time CQIs cannot be calculated. Recall that all UEs compute their corresponding CQIs no matter whether the data are or are not addressed to them.

Firstly, we are going to analyze the CQI distribution for ideal channels (only path losses due to the distance are considered according with LOS or NLOS models). The scenario corresponds to Fig. 1 (a.1). Fig. 2

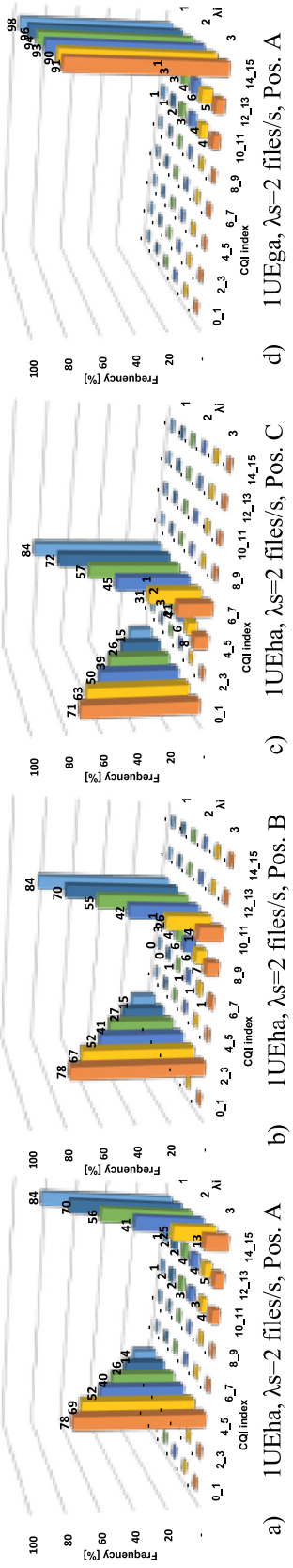

Fig. 2. CQI distributions for UEha and UEga with ideal channel conditions.

shows the CQI distributions obtained from UEha when two LAA eNBs out of mutual sensing range are considered. Results are obtained from different positions (A, B, and C), when the FTP traffic from the server eNB (λs) remains constant (in this case λs is equal to 2 files/second), and traffic from interferer eNB (λi) variates. Recall that position A is closer to the server eNB, meanwhile position C is farther from server eNB. Additional to UEha, server eNB and interferer eNB have 9 and 10 UEs respectively, which are randomly and uniformly distributed around the center of each cell. Table 1 summarizes the simulation parameters, according to the system model described in Section 3.

Fig. 2 (a), (b), and (c) show the CQI distribution for UEha during all simulation time. This node, located in the hidden area, has a bimodal distribution of CQIs that is representative of its dual condition. The lower band of CQI indexes corresponds to collisions (CQIcollision) and the higher band of CQI indexes matches a free collision reception (CQIfreecollision). In general, the severity of the collisions is illustrated in the way as the CQIcollision values span in the lower part of the distribution diagram as shown in graphs (a) CQI=4-5 weak collision, (b) CQI=2-3 medium collision and (c) with CQI=0-1 strong collision. In the same way, the position of CQI values in the CQIfreecollision band, also gives an idea of the channel reception conditions associated to losses due to path attenuation, over an ideal channel (a) CQI=14-15 small path losses, (b) CQI=10-11 medium path losses, (c) CQI=6-7 strong path losses. The distance between the mean of CQIcollision and CQIfreecollision values is related to the difference of received powers from the serving and interfering eNBs. In contrast, Fig. 2 (d) depicts the CQI distribution for UEga in position A, which has a unimodal distribution in contrast with its counterpart in Fig. 2 (a), showing how the channel is not affected by interference.

In summary, from these results, we can say that collisions are reflected in the lower part of CQI distribution and we can define a truncated CQI histogram (TCQI) to reflect the frequency of collisions. TCQI is defined as:

$$TCQI(L) = \sum_{i=0}^{i=L} NCQI(i)$$

where i is the CQI index number (i variates from 0 to 15), NCQI(i) represents the frequency for a CQI with index i, L characterizes the upper CQI index limit that is associated to collisions and $TCQI(L)$ is the frequency of the truncated CQI histogram.

Focusing our attention in the CQI distribution when CQI index ≤ 5, we can note that there is a correlation between the COT (Channel Occupation Time) of interferer node and the value of TCQI [23,24]. To illustrate it, Fig. 3 (a) complements the results of Fig. 2 and compares (when UEha is in position B) the COT in the DL of interferer eNB node with the TCQI values obtained from Fig. 2 (b). Similarly, Fig. 3 (b) exhibits the COT when a Wi-Fi AP is considered as interferer node and compares it with TCQI for the case that exist 1UEha in position B. In this case only DL traffic is enabled for the AP. In both cases the traffic λs remains fixed and equal to 2 files/second and traffic λi varies in the range [0.5, 3] files/second. This correlation exists for all traffic combinations that have been simulated in the three different positions.

In summary, under ideal channel conditions, we can conclude that a bimodal distribution of CQI is an indicative of the existence of a hidden terminal problem. The lowest CQI values represent collisions, and its percentage value gives an estimation about how much traffic is generated by the interferer node.

Now, we are going to obtain the same measurements as Fig. 2 portraits, but in this case we will use a realistic channel, considering shadowing and fading effects due to movement of UEs. The UEs move randomly as described in Section 3. Our reference test nodes (UEha and UEga) are located initially in positions in A, B and C, each one over hidden area and good area respectively, as shown in Fig. 1 (a.1) with 1 UEha. Now, Fig. 4 (a), (b) and (c) show that the clearly visible bimodal distribution for ideal channel (excluding shadowing/fast fading) is almost vanished for the three positions. Comparing the CQI distribution

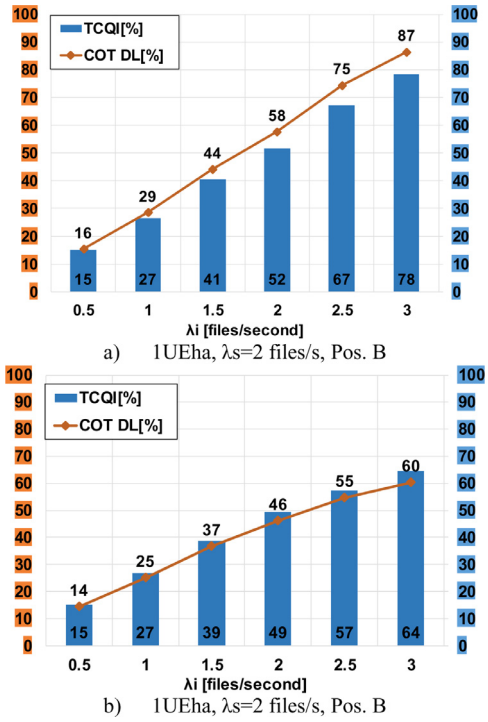

Fig. 3. Truncated CQI and interferer's node. (a) Interferer is a eNB scenario Fig 1 (a.1), (b) Interferer is an Wi-Fi AP scenario Fig. 1 (b.1).

for UEga in position A Fig. 4 (d) with its counterpart in Fig. 2 (d), now, the UEga presents an almost-like Rayleigh distribution of CQIs (in this case, with standard deviation of 4), whereas UEha's CQI distribution presents a clear dispersion along all the CQI indexes as a result of the own dispersion of the two modes identified in the ideal channel. In any case, although these results show that the CQI distribution by itself may not be enough to identify the presence of hidden nodes, there are some features that can be grasped from TCQIs. Let's see what happens when comparing TCQI(L) for UEga and UEha for realistic channels. Based on the results obtained for the case of ideal channels, the TCQI is computed for L=5.

Fig. 5 shows the TCQI(5) percentage values computed in the UEga located in free contention zone in positions A, B, and C, for λs=2 files/second and several interfering traffic loads (λi). As UEga is in free contention zone, the receiving signal in this area is affected mainly by the noise and random losses due to the distance, lognormal and multipath effect inherent to the channel. For each position, TCQI remains almost constant as long as traffic λi gets increased. It only increases slightly, showing that the influence of the remote interferer eNB is minimal. In Fig. 5, the position A shows percentages around 10%, position B around 20% and position C (where the influence of the problematic channel is stronger) around 34%.

In summary, the TCQI distribution obtained from UEga allows to grasp an idea about the channel state in the border cell. In this scenario, values around 10% indicates the UE is just starting to feel the influence of a bad channel, meanwhile a value of 35 % determines a limit for the cell coverture.

The next step is to evaluate how TCQI distribution variates for UE located in hidden areas. Fig. 6 shows the TCQI(5) percentage values (L=5) coming from UEha and compares them with the COT of the interferer eNB. The results depicted in Fig. 6 (a), (b) and (c) are obtained, respectively, for positions A, B and C, for λs=2 files/s and different values of traffic λi, when the scenario has only one UEha in the hidden area as shown in Fig 1 (a.1). In all the cases, it is possible to appreciate that the TCQI distribution correlates with the COT of the interferer.

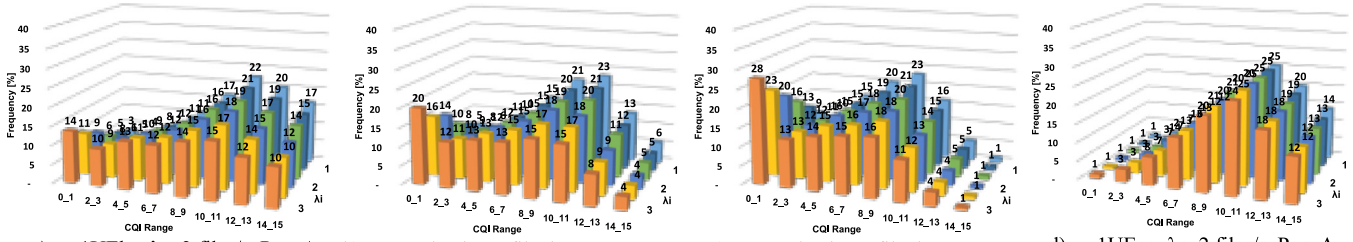

Fig. 4. CQI distributions for UEha and UEga with ideal channel conditions.

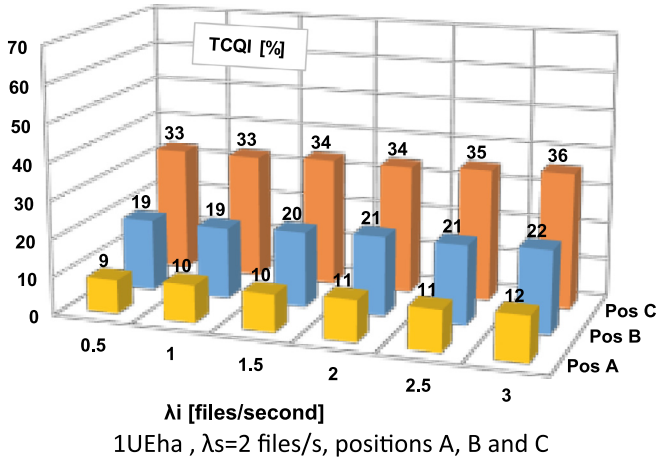

Fig. 5. TCQI(5) percentage for UEga.

Next row, Fig. 6 (d), (e) and (f) correspond to the case when 2 UEha are located on hidden area as shown in Fig. 1 (a.2), each UEha belongs to different network operator. In this case, it is also possible to see that the TCQI histogram correlates with the COT of the interferer eNB. Besides, the figures permit to appreciate clearly that the COT of the interferer node is increased compared with Fig. 6 (a), (b) and (c). This happens because the presence of a second UEha generates more collisions, which originates more errors and consequently more retransmissions for both eNBs. That is, the interferer eNB is also affected by the need of providing service to its own UEs located in the hidden area, which are also affected by the interference generated by the eNB that we evaluate as server. All of this, in short, means a higher COT for interferer and server eNBs. This snowball effect can produce that the scheduler assigns an excessive amount of radio resources to UEha(s) in detriment of other UEga belonging to the cell.

It must be noted that in all the cases the TCQI values for UEha are higher than those obtained for UEga under similar channel conditions. In fact, values for UEha are the result of a lineal combination of those obtained by UEga due to bad channel conditions (almost constant as long as λi grows up) plus the effect of collisions over the transmitted signal. In summary, we can conclude that by setting an appropriate threshold for the TCQI value, we can at least discriminate the UEha whose transmission is becoming to be affected by the hidden node presence (due to interference and COT), regardless of their own channel conditions, and UEga affected by smooth bad channel conditions.

The same analysis can be performed when the interferer node is a Wi-Fi AP. Fig. 7 (a), (b) and (c) illustrate the TCQI values coming from an UEha located in positions A, B and C, when the AP is the interferer (the scenario corresponds with configuration of Fig. 1 (b.1)). In this case, only the traffic in DL is enabled, λs is equal to 2 files/s and λi varies from 0.5 to 3 files/s. Here, as in the previous LAA-to-LAA case, is possible to appreciate that the TCQI values follow the same trend as the COT of interferer. Fig. 7 (d), (e) and (f) show the TCQI values for UEha when there are 2 devices in the hidden area: 1 UEha and 1 STAha. In this case, we can realize that the presence of STAs in the hidden area implies lower AP's COT regarding their counterpart in Fig. 7 (a), (b) and (c). This is because the collisions, which affect to STAha, increase the CW linked to backoff.

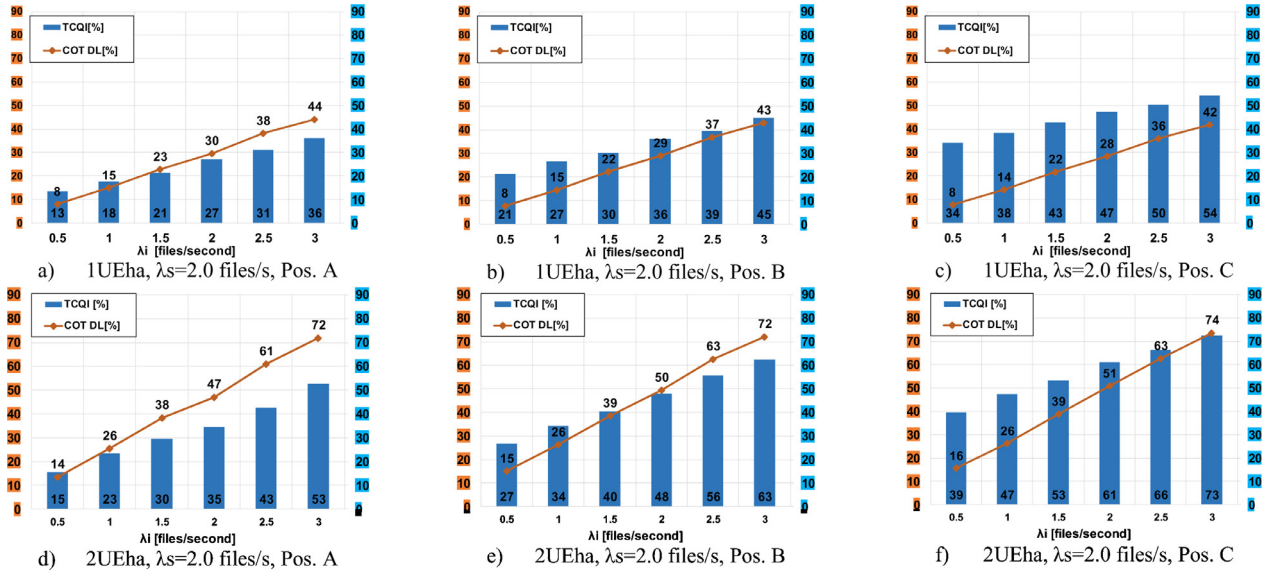

Fig. 6. TCQI(5) percentage. Case LAA-LAA (a), (b) and (c) there is 1 UEha scenario Fig 1 (a.1). In (d), (e) and (f) there are 2 UEha scenario Fig. 1 (a.2).

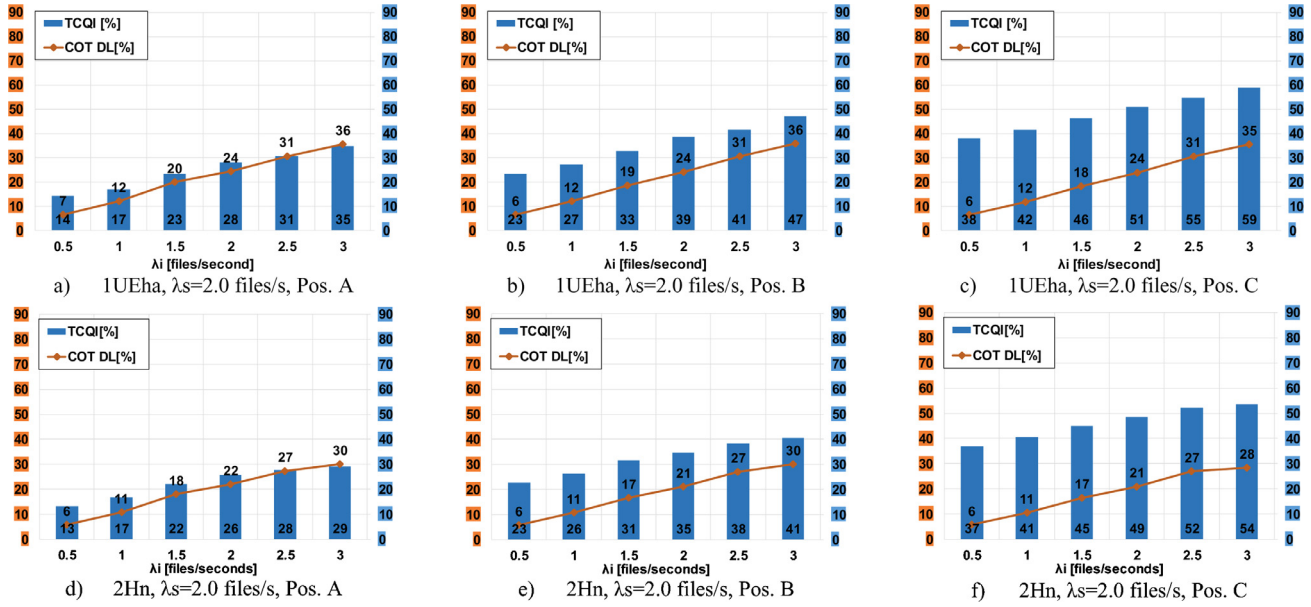

Fig. 7. TCQI(5) percentage. Case LAA-WIFI (a), (b) and (c) there is 1 UEha. In (d), (e) and (f) there are 2Hn (1 UEha and 1 STAha). AP traffic is DL only.

Additionally, something else captures our attention. Fig. 7 (d), (e) and (f) are equivalent to Fig. 6 (d), (e) and (f) because, in both cases, interferer eNB or AP have UE/STA in the hidden area. Wi-Fi and LAA applies similar access methods to ensure coexistence on unlicensed channels, but the results are completely different. This is explained due to the better performance of scheduling in LAA and because the CW (linked to backoff) of LAA will not evolve in the same way as CW of Wi-Fi. In LAA, in order to increase the CW, the received NACKs must be greater than 80%, which may be hard to meet even in the evaluated scenarios.

It is clear that global conclusions obtained for the scenarios LAA-LAA are applicable to LAA-Wi-Fi. Thus, by setting an appropriate threshold for the TCQI value we can detect UEha, regardless of their own channel conditions. However, UEga affected by very bad channel conditions cannot clearly be discriminated from UEha. Thus, we need to explore additional metrics to be considered in addition to TCQI.

4.2. RSRP, RSSI and RSRQ

Other parameters that can potentially be used or combined to reveal the effects of collisions over LAA networks during data transmission are physical measurements reported by UE, according with eNB configuration, as RSRP, RSRQ and RSSI. First, we define these parameters and then, we discuss the potential use. Definitions refer to Resource Element (RE) Section 6.2.2 in [4], which is one subcarrier per one OFDM symbol, and to RB, which is the smallest resource unit that can be scheduled for an UE and it is composed by 12 subcarriers/REs in the frequency domain along a slot in time.

As detailed in [25], the RSRP is defined as the average received power over REs that carry cell reference signals (CRS or RS). That is:

$$RSRP = \frac{1}{N_{RB}} \sum_{k=0}^{N_{RB}-1} \left(\frac{1}{N_{RS}} \sum_{m=0}^{N_{RS}-1} P_{RS}(k,m) \right) \quad (1)$$

where, $P_{RS}(k, m)$ represents the received signal power on the RE m into the RB k, which correspond to the power of one RS (RB contains RSs located over control and data channel) and N_{RS} is the number of REs carrying the RS in a RB. In this case, the average has been performed in a time interval that contains N_{RB} RBs.

The RSSI is defined as the linear average of the total received power (in [W]) observed only in OFDM symbols containing RS, e.g. for antenna port 0 (OFDM symbols 0 and 4 in a slot) and in the measurement bandwidth:

$$RSSI = \sum_{k=0}^{N_{RB}-1} \left[\frac{1}{S} \left(\sum_{s=0}^{S-1} \sum_{r=0}^{SC-1} (P(k,s,r) + I(k,s,r) + No(k,s,r)) \right) \right] \quad (2)$$

where, N_{RB} represents the total number of RBs, S is the number of OFDM symbols carrying RS into a slot (equal to 2), SC is a constant equal to 12 and represents the number of subcarriers in a RB. $P(k, s, r)$, $I(k, s, r)$ and $No(k, s, r)$ denote respectively the received power coming from serving cell, the interference and noise powers of the RE that belongs to OFDM symbol s inside RB k. The total received power in the UE includes all sources: co-channel serving and non-serving cells, adjacent channel interference, thermal noise etc.

Finally, the RSRQ, computed over the same slot interval, is defined as:

$$RSRQ = \frac{(N_{RB} * RSRP)}{RSSI} \quad (3)$$

where N_{RB} is the number of RBs in the RSSI measurement bandwidth of the E-UTRA carrier.

Now, the objective is to analyze the impact that interference has over the values reported by these physical parameters under different load conditions in the server and interferer cell. At the end, the aim is to evaluate if they can be used to detect the existence of hidden terminal problems.

4.2.1. Analysis of load and interference over measured RSRP/RSSI/RSRQ

Firstly, RSRP measures only the RS power and excludes all noise and interference power. Thus, RSRP is a purely coverage-based (Path Loss) parameter which is ideally independent of the network load (own cell load and neighbor interferer cell). By setting an adequate threshold, RSRP provides enough information to the eNB to classify a UE as cell edge or cell inner user. RSRQ can be a potential metric in order to estimate the noise and the interference observed in RE data. However, RSRQ does not correspond with SINR. Defined from RSRP and RSSI, the RSRQ reacts to load changes in both the server cell and the neighboring interferer nodes (eNBs or Wi-Fi). Thus, the meaning of the variation range needs to be known.

Under ideal conditions, when channel is not affected by noise and interference, RSRQ varies between [-10.79, -3.01] dB, depending on the cell load. In the particular case when the cell is not loaded, for every

OFDM symbol that carry RS there are 2 RSs per RB. Then, RSRP is equal to the average of the power of 2 RSs, meanwhile the RSSI is equal to the sum of power of 2 RSs. In this case, it is possible to get the $RSRQ_{No\,load}$ as:

$$RSRQ_{No\,load} = 10\log\left(\frac{1}{2}\right) = -3.01[dB] \tag{4}$$

On the other hand, when the cell is transmitting user data to full load, for every OFDM symbol carrying RSs, the RSRP is equal to the average power of 2 RSs per RB, and the RSSI is equal to the power of 12 REs (2 RSs + 10 REs of user data). Note that inside the RB, the RSs and REs have the same density power, being this assumption reasonable according with power allocation defined in the standard. If we neglect the effect of noise and interference, then the $RSRQ_{Full\,load}$ is equal to:

$$RSRQ_{Full\,load} = 10\log\left(\frac{1}{12}\right) = -10.79[dB] \tag{5}$$

Hereafter, in order to determine the global effect of channel, mobility and interference over signals transmitted by radio bases to UEs over their RSRQ metric is necessary to stablish a mechanism that reflect their overall effect over the received signal. Although RSRQ does not represent SINR, as both metrics are connected, we consider that a relationship can be done by setting a SINR margin (*marSinr*), which we will associate to the corresponding RSRQ values depending on load conditions. RSRQ values associated to a SINR under this threshold are going to be evaluated as UE facing interference (collisions), while RSRQ values above this margin are associated to UEs facing weak or free interference condition. SINR margin selection criterion will be described later.

Let be SINR the ratio $S/(I+No)$, where I and No are the interference and noise that are affecting to REs, respectively, and S denotes the average useful power coming from server node in the same set of REs. Then, if SINR ratio is lower than marSinr, it implies that the received signal is affected by collisions. This consideration is true while the UE is inside the cell's coverture, then:

$$\frac{S}{(I+No)} \leq marSinr \rightarrow There\,is\,collision \tag{6}$$

If marSinr is given in dB:

$$(I+No) \approx 10^{-\frac{marSinr}{10}} * S \tag{7}$$

Additionally, considering that $P_{RS} = P_{RE}$ and similar average conditions for all RBs (being N_{RB} the number of RBs on the measurement bandwidth), we have that RSRQ is:

$$RSRQ = \frac{N_{RB}.P_{RS}}{\left\{(\delta)\sum_{k=0}^{N_{RB}-1} P_{RE}(k) + 12\sum_{k=0}^{N_{RB}-1}[I(k)+No(k)]\right\}} \tag{8}$$

where, δ is the average number of REs per RB that are used as RS or utilized to transmit user data over a OFDM symbol. δ varies between 2 and 12 ($2 \leq \delta \leq 12$). If $\delta = 2$, the cell transmits only RS ($RSRQ_{thNoLoad}$) and when $\delta = 12$, the cell transmits to full capacity ($RSRQ_{thFullLoad}$). Then, considering that the average level of interference and noise per RE is equal for all REs, we compute RSRQ as:

$$RSRQ = \frac{N_{RB}.P_{RE}}{(\delta).N_{RB}P_{RE} + 12N_{RB}(I+No)} \tag{9}$$

Using (7) in (9).

$$RSRQ_{Th} = \frac{1}{\delta + 12.\left(10^{-marSinr/10}\right)} \tag{10}$$

where $RSRQ_{Th}$ represents a RSRQ threshold linked to marSinr for several cell load conditions. RSRQ values below this threshold can be judged as being affected by collisions or interference.

Table 2 shows the expected values of $RSRQ_{Th}$ for different values of marSinr (linked to UEs affected by appreciable interference levels) when δ is equal to 2 ($RSRQ_{ThNoLoad}$) and 12 ($RSRQ_{ThFullLoad}$).

Evaluating the results from Table 2, we can see that depending on the value of marSinr selected the $RSRQ_{ThNoLoad}$ variates significantly from [-12.33, -8.31] dB. Something similar happens with $RSRQ_{ThFullLoad}$. It variates from [-14.33, -12.25]. Additionally, considering together the range of RSRQ values in the absence of interference and the values of the RSRQ from Table 2, we can identify 3 ranges. For instance, considering marSinr=2. The first range corresponds to RSRQ metrics associated to UE free of collisions, in this case the RSRQ falls in [-9.81, -3.01] dB range. In the second range [-12.92, -9.81] dB, the $RSRQ_{Th}$ variates dynamically in function of the cell load, in such a way that if $RSRQ > RSRQ_{Th}$ the UE is considered almost free of interference, otherwise, it is just starting to feel some degree of interference. Finally, in the last range (when $RSRQ < -12.92$) the UE is considered to be affected for different degrees of severe interference. As the marSinr allows to adjust the sensibility of collision detection algorithm, a tuning process will be done to find an optimal value for this margin.

Table 2
RSRQ thresholds for different marSinr and cell loads.

marSinr[dB]	$RSRQ_{ThNoLoad}$[dB]	$RSRQ_{ThFullLoad}$[dB]
4	-8.31	-12.25
3	-9.04	-12.56
2	-9.81	-12.92
1	-10.62	-13.33
0	-11.46	-13.80
-1	-12.33	-14.33

4.3. Practical UE measurements issues

Until this moment we have analyzed how instantaneous RSRP and RSRQ values are obtained in LTE-LAA networks, and also we have defined a $RSRQ_{Th}$ over an average RB used as a reference, which helps us to predict if a UE is facing some degree of interference based in the comparison of the current RSRQ value with the $RSRQ_{Th}$.

According to [26] Sections 9.1.4 and 9.1.7, RSRP is reported by UE PHY layer in dBm, while RSRQ in dB. The values of RSRP and RSRQ are provided to higher layers on a periodic basis (according to configurable reporting intervals of 120ms to 60 minutes as defined in [27]), which in our case is set to 200 ms. Note that low intervals (200ms/400ms) are usually considered in order to provide support to other radio procedures such as cell (re) selection and handover processes. In this way, the UE measurement reports can support the proposed hidden node detection algorithm and follows the same updating rate as the measurements for selection and mobility management processes.

Layer 1 filtering is performed by averaging the instantaneous RSRP and RSRQ obtained during subframes 0 and 5 over OFDM symbols that carry RS, inside a measurement time window of 200 ms. Therefore, if during the window W values of RSRP and RSRQ have been measured, the averaged values are:

$$RSRP_{avUeMeas} = \frac{1}{W}\sum_{i=0}^{W-1} RSRP(i) \tag{11}$$

$$RSRQ_{avUeMeas} = \frac{1}{W}\sum_{i=0}^{W-1} RSRQ(i) \tag{12}$$

where RSRP(i) and RSRQ(i) are the individual averaged linear magnitudes measured in the i-th subframe 0 and 5 over all RBs that belong to the same TTI.

Applying (12) in (10) and considering that δ represents the number of REs used to transmit RS and user data up to a maximum of 12 REs, the average RSRQ threshold ($RSRSQ_{avTh}$) in logarithm units can be represented as:

$$RSRQ_{avTh} = -10\log\left(2 + 10\frac{K_{used}}{K_{total}} + 12\left[10^{-\frac{marSinr}{10}}\right]\right) \tag{13}$$

where $0 \leq K_{used}/K_{total} \leq 1$ characterizes the ratio between the number of REs that are transmitting data (used) and the number of REs available for data (total) that are contained on OFDM symbols that carry RSs.

Table 3
Parameter definitions for DCD algorithm.

Parameter	Description
CQI	UE's CQI indexes reported
TCQI	Truncated CQI histogram
TCQIMin	Truncated CQI histogram minimal threshold. Values under this threshold represent smooth bad channel conditions
TCQIMax	Truncated CQI histogram maximal threshold. Values above this threshold represent different levels of bad channel conditions.
RSRQavUeMeas	Average RSRQ value obtained from UE report
RSRQavTh	Average RSRQ threshold obtained as defined in formula (13)
RSRPavUeMeas	Average RSRP value obtained from UE report
RSRPThr	This RSRP threshold represents the RSRP for which the UE is inside the cell's coverture. UE with RSRP higher than this threshold is inside the cell's coverture, otherwise the UE is in handover zone.
UeCol	If this flag is set to 1, then a collision has been detected
PrbTx	Number of PRBs used by eNB to send data to specific UE.
Kused	Total number of PRBs transmitted from a specific eNB to their UEs during UE measurement report period.
Ktotal	Total number of available PRBs during UE measurement report period.
α	Compensation factor for approximation from REs to RBs.
UeHa	If this flag is set to 1, then UE is judged as located in hidden area

Assuming that the minimum level of granularity at PHY layer is the RB (and not REs), a good approximation is to replace K_{used} by the number of RBs used to transmit user data and K_{total} by the total number of RBs during last 200 ms.

It is important to note that RSRQ measurements obtained by an UE are reported to the eNB independently if the scheduler has assigned or not radio resources to this particular UE. RSRQ measurement is an average value over the entire band and decoupled of the level of CQI.

In general terms, we can conclude that RSRQ permits to know if the UE is located or not in a zone of interference. If an UE observes good RSRQ and a high concentration of lower CQI indexes, statistically speaking, it is reasonable to presume that this behavior is motivated by bad channel conditions. In other hand, if the RSRQ is bad, the correlation with the RSRP level is important. In summary, a bad RSRQ associated with a good RSRP level together with a high concentration of bad CQIs must be related to non-predictable interference (i.e. interference coming from hidden node). If the level of RSRP is acceptable, but if the UE is located in the cell's limit, the assessment about the existence of hidden nodes is similar but the appearing of errors due to the channel along with the effect of interference may change the decision thresholds.

5. Hidden node detection algorithm

Starting from results obtained in Section 4, we propose a Dynamic Collision Detection (DCD) algorithm which makes use of CQI distribution, mapped on a TCQI value, RSRP and RSRQ metrics obtained from UEs. This algorithm makes feasible the detection of collisions that affect UEs over a dynamic channel on LAA networks when the device is positioned on the hidden area. DCD adapts itself dynamically, so it is able to detect collisions anytime the measured RSRQ falls below a RSRQ threshold allowing to generate a response as fast as the duration of the UE measurement report window. This information can be used to make decisions about if it is convenient that an UE should remain on the unlicensed band or is better to be assigned to licensed one. Table 3 displays the parameters that compose the DCD algorithm.

The proposed solution is uncoordinated, because in practical deployment scenarios is difficult to find a coordinated solution between different operators. On the other hand, it tries to minimize the required signaling overheads between eNB and UEs. The DCD algorithm is tested over different scenarios with variable traffic loads, a realistic channel, which considers different variables such as LOS, NLOS, lognormal and multipath losses, and UEs in movement within different positions inside/outside the hidden area all over the band of 5 GHz.

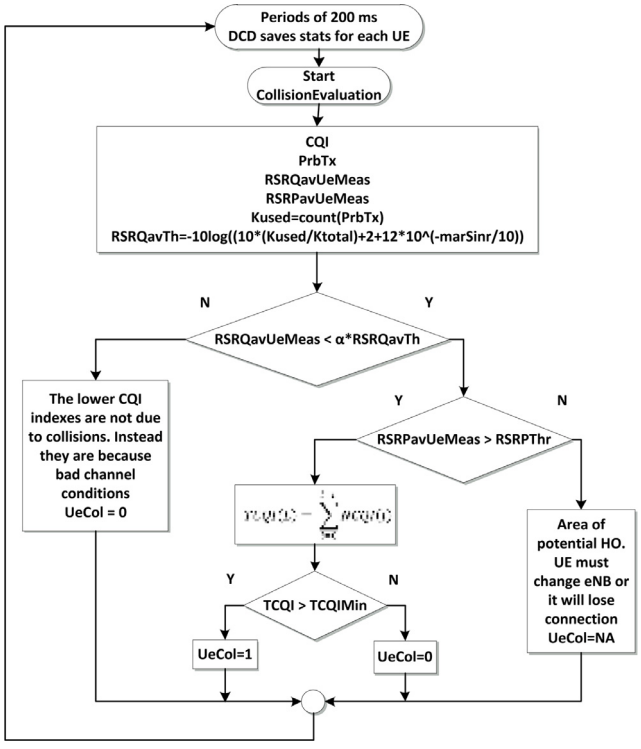

Fig. 8. DCD Algorithm.

Fig. 8 shows the flow chart for the DCD algorithm. According with previous analysis, the two main metrics to evaluate collisions are CQI and RSRQ, which will be correlated with RSRP and cell load statistics. The DCD algorithm saves the statistics generated for every single device attached to the eNB. They are saved periodically every 200 ms and are used to predict if the signal has suffered some kind of interference.

The current RSRP and RSRQ values are obtained from UE physical layer measurement reports, according the reporting configuration set by the RRC and notified by the eNB to the UE. The CQIs are generated following a wideband and periodic criterion where network notifies UE via DCI to transmit the report every 2 ms. The reason behind this time interval is to assure that the CQI measurement is done inside the duration of a LAA frame, which lasts a TxOP. Considering the minimal TxOP de-

fined in the standard equal to 4 ms, the selected time of 2 ms fulfills this requirement. Also, as agreed on RAN1 LAA ad hoc meeting, *"Interference measurement for CSI is not allowed outside of the serving cell transmission period"* on an unlicensed carrier [28,29], which means that all CSI measurements must be done during transmission of DRS or user data, if none is transmitted by eNB, the UE must not make measurements.

Now, let's see the basis of the algorithm. As illustrated in Section 4, we can conclude that by setting an appropriate threshold for TCQI values, we can at least discriminate UEha whose transmission is significantly affected by the hidden node presence (due to high interferers COT), regardless of their own channel conditions, and UEga affected by very bad channel conditions. As shown in Fig. 5 of UEga, the truncated CQI histogram for UEga has an almost constant value for different values of traffic λi and only depends on the average quality of the channel. In the evaluated scenario, and using TCQI(5) with L=5, UEga in position C (limit of coverage) has a TCQI around 35% because is the farthest and it is affected by the worst quality channel. Meanwhile, the UEga located in A, which is just starting to perceive the influence of bad channel, has a TCQI around 10%.

Regarding to UEha, its TCQI value depends on two variables, the first is correlated with COT of interferer node, and the second comes from its relative position over the border cell as the case of UEga. In general, UEha whose service is severely affected by the interference (COT is high enough) computes TCQI higher than those reported by UEga in the worst quality channel, no matter their own channel conditions.

Thus, we propose two thresholds for TCQI (*TCQIMin* and *TCQIMax*) in order to discriminate UEga affected by several degrees of channel degradations and UEha affected by interferences.

TCQI values lower than *TCQIMin* are associated to UE facing smooth bad channel conditions or poorly affected by interference of hidden nodes. On the other side, a UE with a TCQI higher than *TCQIMax* is supposed to be affected by strong bad channel conditions (i.e. UEga in position C) or moderate to strong interference (UEha). Whereas, UE whose TCQI range is between TCQIMin ≤ TCQI ≤ TCQIMax is listed as a UE facing bad channel conditions (i.e. UEga located in position B) or moderate to strong interference. Contrary to UEga, we can stablish that a UEha in the evaluated scenario will start to feel appreciable effects of collisions when its TCQI becomes higher than TCQIMin.

The proper selection of the values of TCQIMin and TCQIMax is a relevant issue, which may be based on learning about historic statistics. According with results previously obtained for the simulated scenarios and UEga, TCQIMin can be set to 15%, whereas TCQIMax has been set to 35%. Nevertheless, as we refer above, we know that TCQI based detection could be dependent on the scenario and may not provide enough discrimination between UEs affected by bad channel conditions and UEha. Thus, the assessment is first based or reinforced through another filter based on RSRQ and RSRP measurements. Now, the matter is how to adequately set the *RSRQavTh* value or better how to adequately set the marSinr it depends to. In fact, RSRQavTh may change dynamically in each period of evaluation, because, as defined in section 4, it depends on the average load of the cell.

Consequently, if the reported *RSRQavUeMeas* of UE is higher than RSRQavTh (defined according Eq. (13)), the number of lower CQIs indexes attained to the UE are assumed statistically due to poor channel conditions rather than high interference, at which case the *UeCol* is set to 0. But, if the RSRQavUeMeas is lower than the RSRQ average threshold, further analysis is required in order to evaluate if the UE is in the area of potential handovers. In this case, no matter the UE is affected by hidden nodes or not, it probably need to perform a handover. Thus, if RSRQavUeMeas is lower than RSRQavTh, the algorithm considers RSRP measurements. UEs with *RSRPavUeMeas* higher than a threshold *RSRPThr* are tagged as holding on the cell. The case when RSRP is lower than RSRPThr is not considered because when the UE has overpassed this lower limit it should have done a handover to next cell or it is almost to lose connection with its radio base. In this case, we have set RSRPThr equal to -113dBm.

In order to make decisions when RSRQavUeMeas is lower than RSRQavTh, it has been stablished one correction factor to compensate some deviations that the use of RBs rather than REs may generate to computer the K_{used} parameter inserted in (13). After a simulation campaign it has been selected α=0.95.

Then, if RSRPavUeMeas is higher than RSRPThr, the algorithm takes the decision about if the UE is affected by collision comparing the current TCQI with the TCQIMin. That is, if TCQI > TCQIMin and RSRQavUeMeas < α^*RSRQavTh the UE is judged as facing collision and the UeCol flag is set to 1.

Note that this part of the DCD process, in order to set flag UeCol, is repeated periodically every 200 ms to every single UE attached to eNB. However, decisions about whether a UE should be classified as significantly affected by hidden node presence cannot be based only in one period of measurement. Through the analysis of the data along several consecutive measurement periods of 200ms (up to M_A), we can see that over a short time interval, the probability of an UEha for obtaining a second tag as collided (UeCol=1), given that a first collision tag occurred, is higher than the probability of an UEga has been tagged with a second false collision given that a first false collision tag happened. True collisions are concentrated around the time that data are being affected by collisions. This time depends on the file size and it can take various continuous frames. In other hand, false collisions are related to fading or bad channel conditions which occur randomly and they are short in duration.

With this in mind, in order to tag a UE as UEha (flag UeHa=1) DCD evaluates the number of UeCol=1 (NumCol) that occurred inside an interval of M_A consecutive measurement time reports. In this case M_A=4. If NumCol is higher than 2, it sets the UeHa flag to 1, otherwise the flag is set to 0. This last section of the algorithm detects if the UE analyzed is effectively inside a hidden area eliminating almost all errors caused by false collisions.

6. Numerical results and discussion

In this section, we evaluate the performance of the proposed DCD algorithm over different conditions of the LAA-LAA scenario and conditions according to the system model described in Section 3 and simulation parameters summarized in Table 1. Similar general conclusions have been obtained from all scenarios independently of the source of the interference, either eNodeB LTE or AP Wi-Fi. Results when the interference source is an AP have not been included to avoid redundancy. In addition, and as a previous step, we present the results that support the use of RSRP and, RSRQ in the DCD algorithm. As stated before, the statistics comes from UEga and UEha taken as a reference and located in positions A, B and C in the cell's border (see Fig. 1.a).

In summary, the main features applied to the simulations tests are:

- Different number of UEha, 1 or 2 nodes.
- Variable server and interferer traffic load; the traffic is increased from a minimal value to a maximum independently for every eNB.
- Two kinds of traffic, FTP with an arrival time that follows a Poisson distribution, and UDP traffic where a constant bit rate is requested for every UE to its eNB.
- UE mobility with constant pedestrian speed inside a limited area (a circle of limited radius) in order not to change distribution of UEs between good and hidden node areas.
- UEga and UEha are located in 3 different initial positions in the cell border and move slowly around it. Thereby, meanwhile an UEga gets low, medium and high losses because channel conditions, an UEha suffers low, medium and high interference in addition to variable channel conditions. Both reference nodes have the same average distance to the eNB. The data coming from both UEs are compared in order to understand how the channel affects the received signal for UEga and how channel and collisions affect the incoming data for UEha when both nodes are at the same average distance.

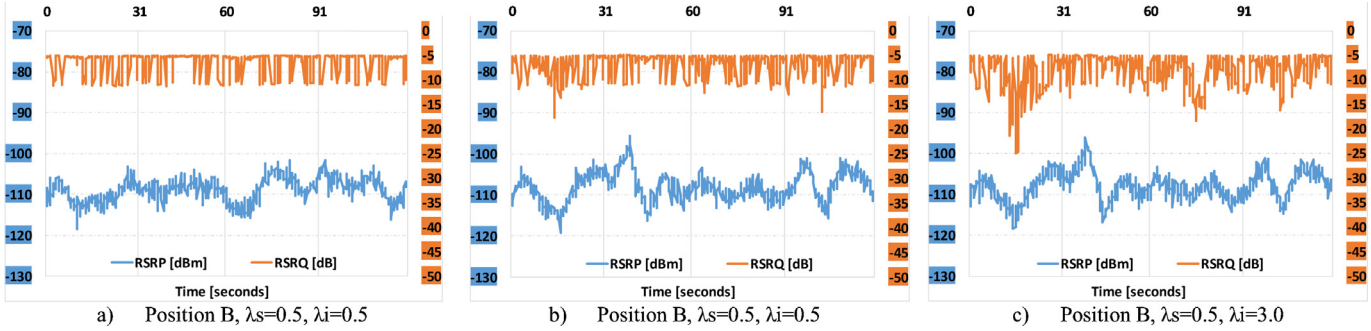

Fig. 9. RSRP and RSRQ vs time. Fig. (a) correspond to measurement reports given by UEga meanwhile Fig. (b), and (c) correspond to measurement reports coming from UEha for traffic FTP (burst type) scenario Fig 1 (a.1) LAA-LAA.

■ A realistic channel affected by lognormal and multipath losses.

6.1. Physical UE measurements

First, we analyze how RSRP and RSRQ values vary. The statistics in which we focus our attention come from references nodes UEha and UEga located in position B, scenario Fig. 1 (a.1) LAA-LAA with 1UEha.

Fig. 9 represents the UEha and UEga measurements reported to its server eNB. Fig. 9 (a) belongs to UEga, while (b), and (c) are from UEha. They show the RSRP and RSRQ vs time, for different traffic conditions. The traffic used is the FTP model described before, with independent traffic rates for server, λs, and interferer eNB, λi, in [files/second]. All subplots correspond to UE located in position B, where λs remains constant and equal to 0.5 and traffic λi variates. For UEga (Fig. 9 (a)), only results for λi=0.5 files/second are included because, as expected, similar results are obtained no matter the λi values. In the case of UEha (Fig. 9 (b) and (c)), results are obtained for low (λi=0.5) and high (λi=3) interfering traffic load. As shown in Fig. 9, in all the cases, RSRP measurements are in the range of [-120, -100] dBm, this is because physically UEha and UEga are located over the cell's border in constant random movement. That is, UE's RSRP is affected by lognormal and multipath losses due the channel and the mobility of the device.

Concerning to RSRQ values, it has been demonstrated in Section 5 that RSRQ varies over [-10.79, -3.01] dB when interference and noise do not have influence over the received signal. As expected, in Fig. 9 (a) the RSRQ variates approximately in the range [-11, -5] dB. Note that the lower level agrees with the result from Eq. (5), meanwhile the higher level is a little different as demonstrated in (4). The reason is because the PDCCH always has control data to transmit and so REs are not always completely empty of data for no load condition. Fig. 9 (b) and (c) show that RSRQ ranges approximately from [-25, -5] dB. The RSRQ decreases as higher the λi traffic. This is because as higher the traffic λi greater the likelihood of collision.

In order to see the correlation between reported RSRP and RSRQ values, Fig. 10 represents the RSRP vs RSRQ plots for UEha and UEga, and the correspondent RSRQ histograms when FTP traffic is considered. Fig. 10 (a), (b) and (c) depict the RSRP vs RSRQ plots for the same value of λs (equal 0.5) and increasing value of λi (0.5, 2 and 3 files/second, respectively). Similar conclusions can be obtained when higher values of λs are evaluated. The UEga and UEha plots are overlaid to get a better visualization of the effect of collisions over the RSRQ metric. In this scenario, where a bursty traffic is considered, these figures show a bimodal distribution for RSRQ no matter the value of RSRP. Additionally, these graphs permit to appreciate how the RSRQ achieves a non-linear response as the RSRP overpass the lower limit of -113 dBm. These results are coherent with RSRQ histograms depicted on Fig. 10 (d), (e) and (f) for UEga and UEha nodes. One mode is centered around RSRQ=-5dB and represents periods of time without interference and almost zero load and the other mode is centered around RSRQ=-11dB and represents a scheduler using all RBs to transmit user data.

However, they show differences between UEga and UEha. For UEga, RSRQ values are scattered between the two limits. For UEha, Fig. 10 (a), (b) and (c) permit to appreciate how the RSRQ value overcomes the lowest limit given in Table 2 when the signal has been affected by collision. Besides, the number of RSRQ representing collisions gets increased as the UEha receives more interference because the higher λi traffic from interferer eNB. Additionally, for UEha, when transmissions are affected by collisions, lower RSRQ values were obtained as lower RSRP levels are. This is because lower RSRP corresponds with higher power values from the interfering eNB.

A similar analysis is performed in Fig. 11 when UDP traffic is considered. In this case, instead of bursty traffic, a constant bit rate (in Mbps) is requested for each UE to its eNB. In this graph, Rs is the target rate that server eNB tries to achieve for each UE (a single UE) and Ri represents the same parameter for the interferer eNB.

Fig. 11 (a), (b) and (c) depict the RSRP vs RSRQ plots for UEga and UEha. The UEga and UEha plots are overlaid to get a better visualization of the effect of collisions over RSRQ metric. In addition, Fig. 11 (d), (e) and (f) show the correspondent RSRQ histograms.

Now, data coming from UEha and UEga do not have the bimodal behavior typical in scenarios with bursty traffic. Here, the scattered points are diffused, showing the different grades of occupancy of REs inside of RBs. Nevertheless, again, there are differences between data received from UEga and UEha. For example, in UEga comparing Fig. 11 (a) with Fig. 11 (b) and (c), and considering that RSRQ is function of used REs. we see that the distributions in Fig. 11 (b) and (c). Have a small standard deviation. The mean reason behind this phenomenon is the high number of retransmissions that a constant and high interference produces over a UEha. Although the interference does not affect the reference UEga, the increment in Ri imply a rise in the effect of interference over other UEs (e.g. the UEga) in the serving cell. The rising interference produces many retransmissions and eNB reaches the full load state. Because of this, RSRQ of UEga, which is not affected by interferences, remains around the minimum RSRQ value (-11 dB), which corresponds to a full load cell case.

When UEha is considered, Fig. 11 shows how, as for UEga, when Ri is increased (Fig. 11 (b), (c), (e) and (f)), the highest expected value of RSRQ is limited to the minimum value (around -10dB) in absence of interference. This is due to the full load condition of the cell as explained above. Nevertheless, contrary to UEga, UEha's RSRQ values get down until -18dB due to collisions. Note that, for UEha, when transmissions are affected by collisions, lower RSRQ values were obtained as lower RSRP levels are. This is because lower RSRP correspond with higher RSRP values from the interferer eNB.

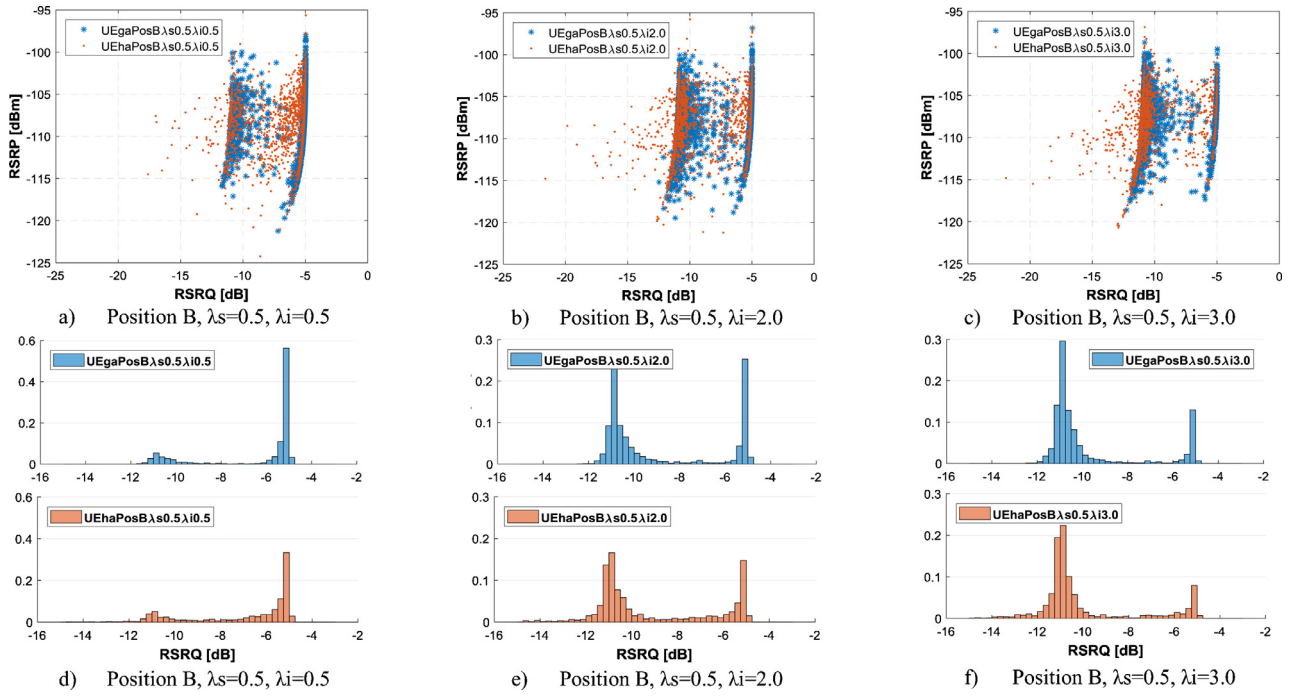

Fig. 10. RSRP vs RSRQ and RSRQ histograms. Fig (a), (b) and (c) show the RSRP vs RSRQ plot for UEha and UEga both nodes are at the same average distance from server eNB (position B), λs is constant equal to 0.5 and λi variates. Fig. (d), (e) and (f) represent the RSRQ histograms for UEha and UEga under same conditions as their counterparts (a), (b) and (c). All UEs are facing FTP traffic, scenario Fig 1 (a.1).

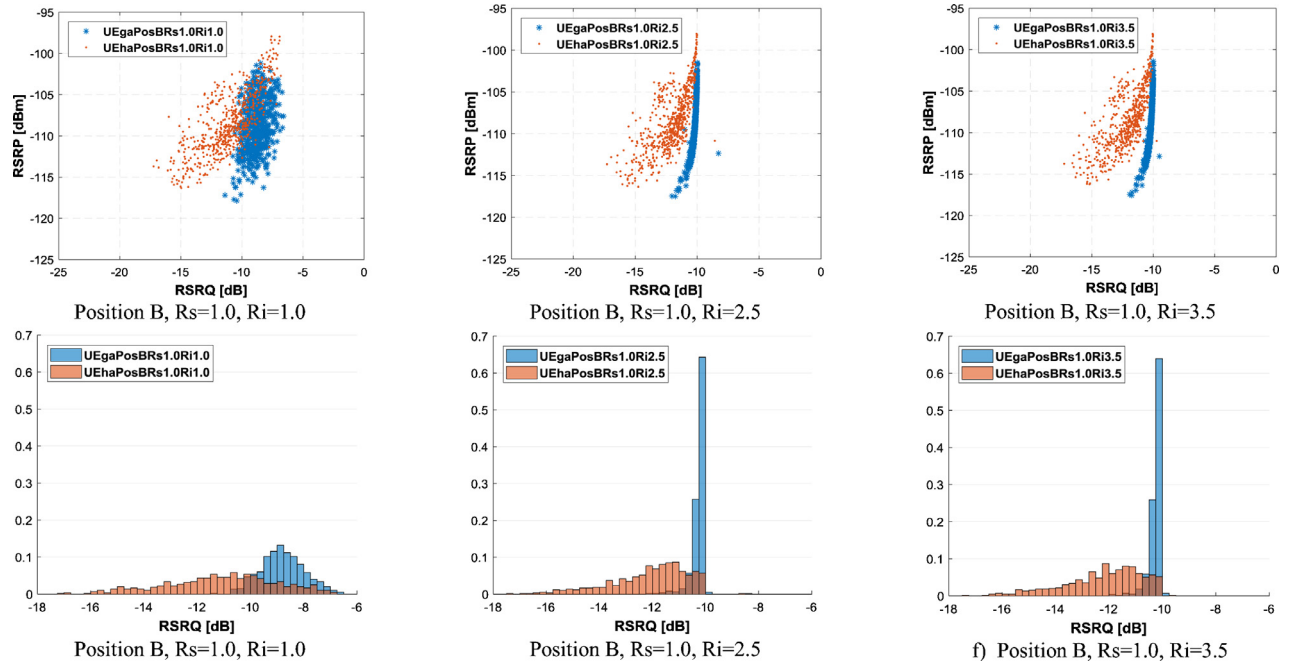

Fig. 11. RSRP vs RSRQ and RSRQ histograms. Fig (a), (b) and (c) show the RSRP vs RSRQ plot for UEha and UEga both nodes are at the same average distance from server eNB (position B). Fig. (d), (e) and (f) represents the RSRQ histograms for UEha and UEga under same conditions as their counterparts (a), (b) and (c). All eNBs transmit CBR traffic where Rs is the server's rate and Ri the interferer's rate in Mbps, scenario Fig 1 (a.1).

6.2. Collision detection results using DCD algorithm

As detailed before, the DCD algorithm is evaluated under different scenarios and conditions in order to test the performance and consistency of results.

Fig. 12 represents the percentage of times a UE is evaluated as under collision (Ncol) by DCD algorithm. For instance, Ncol=0.2 indicates that DCD algorithm has detected that 20% of samples (1 sample is obtained every 200 ms) during all simulation time correspond to collisions. All statistics come from UEha when only 1 UE is in hidden area (1 UEha) scenario Fig. 1 (a.1). The aim is to evaluate the effect of the selected marSinr value under several conditions of traffic in the server and interferer eNB. Results are obtained for bursty traffic scenario (FTP traffic model) with independent traffic rates for server λs and interferer λi.

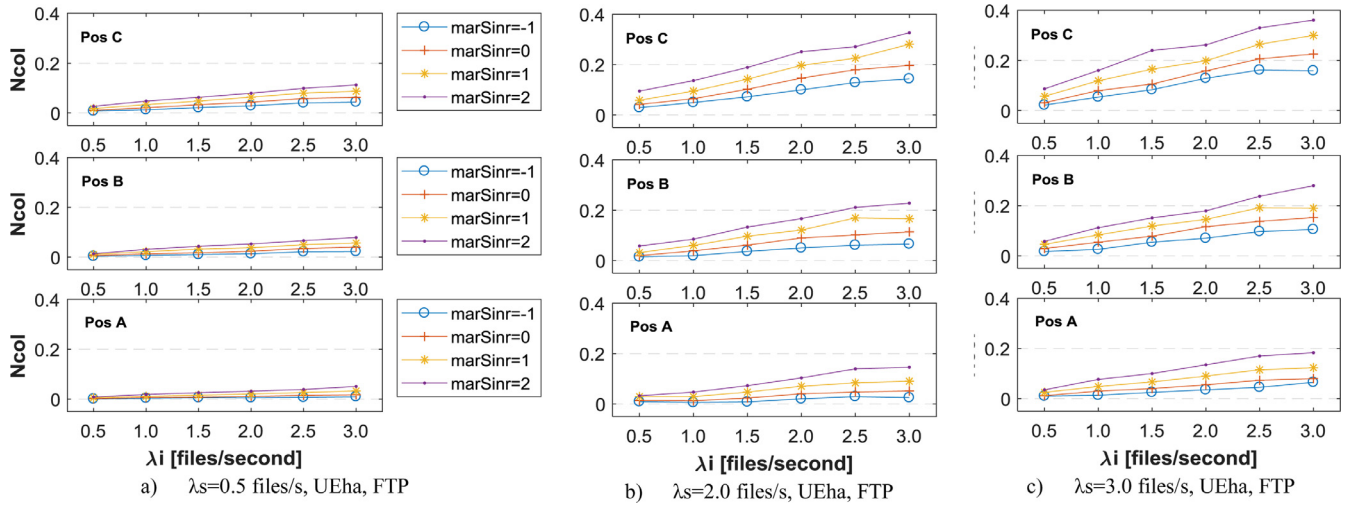

Fig. 12. Number of collisions [%] vs λi traffic for UEha. The traffic λs variates from (a) λs=0.5 files/s, (b) λs=2.0 files/s, and (c) λs=3.0 files/s for traffic FTP, case 1UEha. LAA-LAA.

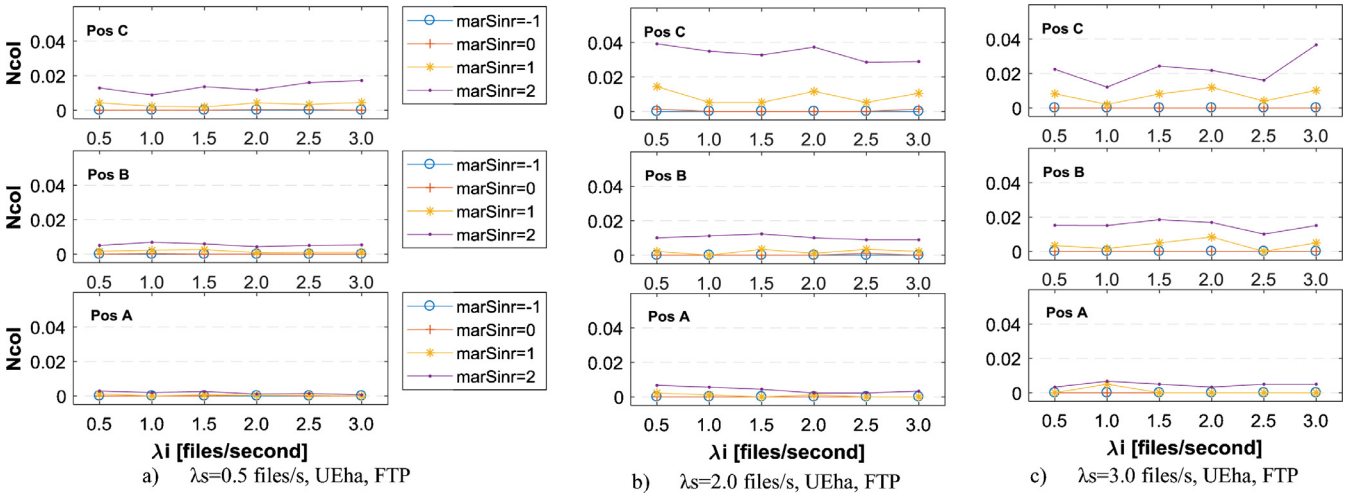

Fig. 13. Number of collisions [%] vs λi traffic for UEga. The traffic λs variates from (a) λs=0.5 files/s, (b) λs=2.0 files/s, and (c) λs=3.0 files/s for traffic FTP, case 1UEha. LAA-LAA.

Fig. 12 has 3 subplots, each one for different values of traffic λs. Fig. 12 (a) depicts the Ncol that UEha faces when λs=0.5, λi gets increased from 0.5 to 3 files/second and for several values of marSinr (-1, 0, 1 and 2). Fig. 12 (a) is subdivided in 3 subplots, the upper subplot corresponds to the case when UEha is located in position C, the middle subplot when UEha is in position B and the lower subplot to UEha located in position A; recall that position A is closer and position C is farther from server eNB. The X axis represents the interferer traffic λi when FTP traffic is applied, meanwhile the Y axis displays the percentage of times a UE is evaluated as under collision. Fig. 12 (b) and Fig. 12 (c) show the same results when λs=2 and λs=3, respectively. Comparing the number of collisions among 3 subplots in Fig. 12 (a), (b) and (c) is possible to see that, as expected, $Ncol_{PosC} > Ncol_{PosB} > Ncol_{PosA}$. This is due to the fact that as the UE gets closer to its eNB, the probability of collision gets reduced.

Additionally, it is possible to appreciate that the Ncol grows linearly as traffic λi and λs also increase linearly. However, the most relevant issue concerns the selected marSinr. The results depend significantly on the level of marSinr assumed, and it needs to be set carefully by comparing results with those obtained for UEga in similar conditions.

Now, in Fig. 13, we evaluate Ncol for UEga in similar conditions than Fig. 12. Theoretically, the number of collisions for UEga should be zero because there is not an interference source nearby the UEga. Nevertheless, factors such as position of UE in the border cell and movement of the UEga makes the UE be evaluated sometimes as in the area of potential handover. Additionally, NLOS propagation path and the realistic channel make the received signal to achieve levels that fall under the limit imposed by marSinr (especially when UE is in the border of the cell's coverture). Thus, when applied the DCD algorithm the weaker received signal can be evaluated as a false collision.

In summary, we can see that the number of false collisions gets increased as we get closer to the limits of the cell's coverture, especially in position C. Furthermore, by imposing marSinr = 2dB, the probability that RSRQ falls below the RSRQavTh is greater, because the probability that the difference of power between the received signal and the interference signal (noise plus interference) becomes lower than marSinr = 2dB is higher. As a result, the DCD algorithm evaluates erroneously the UEga as in collision. As it is reasonable, if higher values of marSinr are selected, the probability of false collision grows in all positions. Additionally, Fig. 13 permits to see that in general marSinr equal to -1 and 0 makes a good job reducing the number of false collision registered for UEga for all combinations depicted in the subplots, choosing these values of marSinr the false collision are reduced almost to zero.

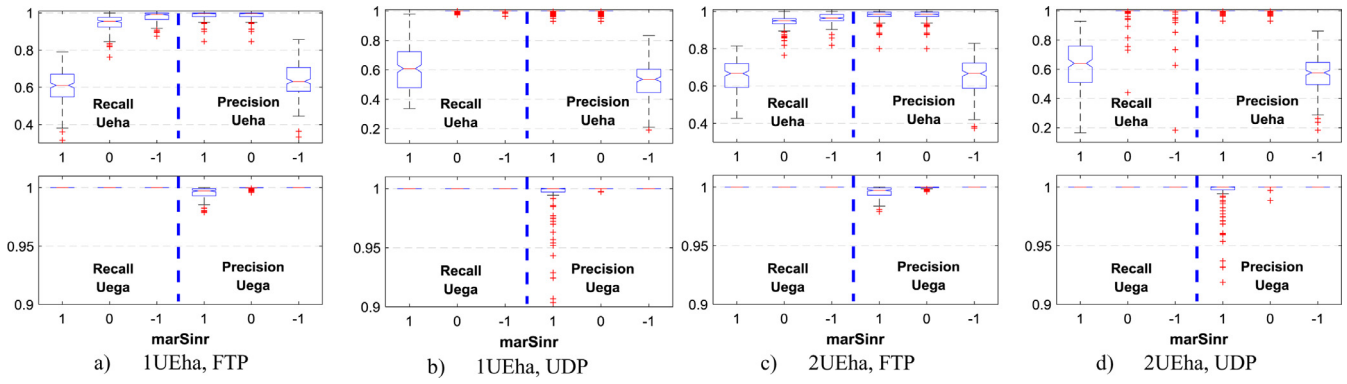

Fig. 14. Recall and Precision. (a) 1 UEha scenario Fig. 1 (a.1) and traffic FTP, (b) 1 UEha scenario Fig. 1 (a.1) and UDP traffic, (c) 2 UEha scenario Fig. 1 (a.2) and FTP traffic, (d) 2 UEha scenario Fig. 1 (a.2) and UDP traffic case LAA-LAA.

Thus, by comparing UEha and UEga results, we can conclude that by setting marSinr lower than 2dB, DCD algorithm detects collisions in UEha and reduces the number of false collision in UEga. Now, in order to choose an appropriate value for marSinr we evaluate the performance of DCD algorithm. We compare the number of collisions decided by DCD and the number of true collisions for marSinr values equal to -1, 0 and 1.

We define that a true collision will occur when server eNB and interferer eNB transmit simultaneously and the difference in power between the received server and the interferer signal in the UEha is lower than a threshold. Ideally, a threshold ≤ 0 dB means that the interferer power in average is at least equal or higher to the average server power inside the analyzed window. In order to minimize problems with averaging powers and consider all interferers that almost reach the server power signal, we consider that a threshold of 2 dB is an acceptable standing point to continue with the analysis.

In other hand, DCD considers both metrics a RSRQ below RSRQavTh, based on marSinr and the TCQI above the TCQIMin threshold in order to evaluate when collisions are happening. In the context of DCD, a collision will occur when the UE located in hidden area detects that both metrics have been overpassed their respective thresholds in the same sample window.

We utilize two metrics known as Recall and Precision [30], which are common metrics used in logistic regression. Logistic regression is a popular algorithm to solve classification problems. Considering that DCD algorithm is a deterministic classifier, we make use of these metrics to evaluate the performance of the algorithm. The metrics are defined as follows.

- Recall: Percentage of collisions correctly detected, among the number of collisions occurred (collisions detected and undetected):

$$Recall = \frac{True\ Positives}{True\ Positives + False\ Negatives}$$

- Precision: Percentage of collisions correctly identified, among all those events classified as in collision:

$$Precision = \frac{True\ Positives}{True\ Positives + False\ Positives}$$

Both metrics range from 0% (poor) to 100% (optimal). Note that high Precision is useful when the classifier achieves good Recall, and vice versa.

Fig. 14 shows the Recall and Precision results for different scenarios. Fig. 14 (a) depicts the results coming from Figs 12 and 13 that correspond to the case when there is 1 UEha and the traffic is FTP. The X axis represents the marSinr value which range from [-1, 1]. Fig. 14 (a) has 2 subplots. The upper subplot shows the outcomes for UEha, while the lower subplot belongs to UEga. It should be noted that, in order to have the global performance, we calculate the average recall from individual recalls coming from all traffic combinations of λs and λi, being

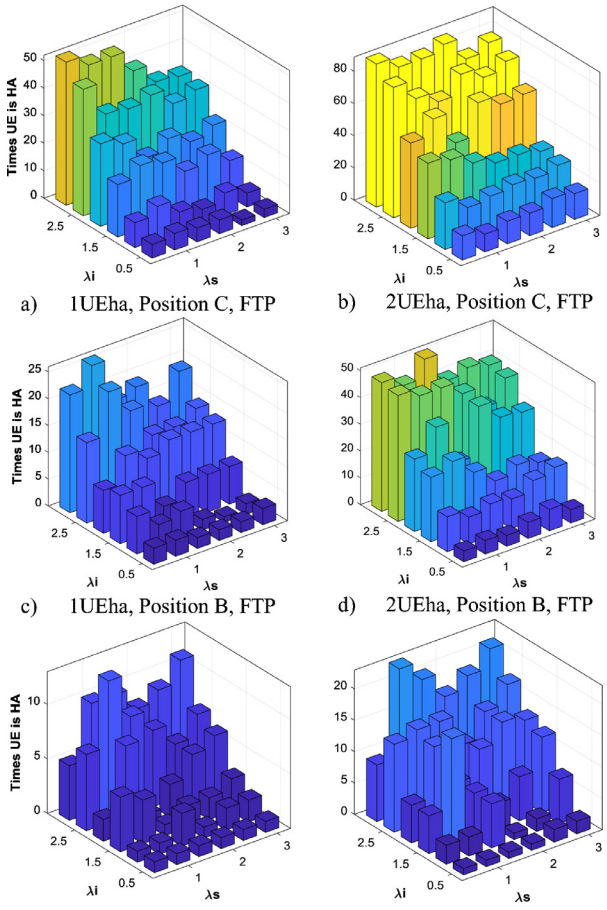

Fig. 15. Number of times that an UE is located in hidden area. Fig. (a), (c) and (e) correspond to scenario from Fig. 1. (a.1) and Fig. (b), (d) and (f) comes from scenario from Fig. 1 (a.2).

they 0.5, 1, 1.5, 2, 2.5 and 3 files/second and all positions combinations (Positions A, B, and C).

Considering that recall and precision are useful when both simultaneously present values near to optimal, it is possible to see that for the case of UEha the best results comes when marSinr = 0, meanwhile for the case of UEga practically all marSinr have good results. Fig. 14 (b) corresponds to the case when traffic presents a constant bit rate (UDP) which ranges [1, 3.5] Mbps when the hidden area has 1 UEha scenario depicted in Fig. 1 (a.1). Fig. 14 (c) shows the results when the traffic is FTP and the hidden area has 2 UEha (scenario Fig. 1 (a.2)), one attached

to server and other to interferer eNBs, and Fig. 14 (d) when the traffic is UDP with 2 UEha (the scenario is the same that the previous one), 1 UEha for every cell.

Evaluating the results of recall and precision for all scenarios displayed on Fig. 14, we conclude that marSinr=0 performs better in average for all combinations in traffic and positions for recall and precision metrics, meanwhile the other marSinr values get good results only in one metric (recall or precision) which does not fulfill the requirements described before.

With marSinr = 0 we can see that recall and precision has a median above 95% for UEha and UEga, which implies that the DCD algorithm classifies in average above the 95% of the time correctly if the UE is facing collisions and almost 100% of the time when the UE is facing only bad channel conditions.

Finally, Fig. 15 shows the histogram of number of times that UE is judged as located inside the hidden area (NumUeHa) according with UeHa flag. Fig. 15 (a), (c) and (e) shows the NumUeHa for scenarios with 1 UEha in position A, B and C. Similar results are obtained in Fig. 15 (b), (d) and (f) for the scenarios with 2UEha for FTP traffic. As expected, in both cases, the NumUeHa is increased as λi gets higher for FTP traffic. Besides, the NumUeHa for case 2UEha is higher than 1Ueha case, mainly because retransmissions on interferer eNB that results on higher COT. It has not been plotted the NumUeHa for UEga because for all cases evaluated the NumUeHa was practically zero for all scenarios and both types of traffic.

7. Conclusions and future work

This work has emphasized its study in finding a solution to detect UEs that are being affected by hidden nodes in LAA network deployments. With this in mind, we have analyzed physical parameters as RSRP/RSRQ, reported by UEs and CQI distribution to deal with this problem. The analysis has been performed over a realistic channel and variable traffic conditions to understand how these parameters are affected by different levels of interference.

We have analyzed analytically the dependence between RSRP, RSRQ and SINR in scenarios facing different levels of interference. We have found an analytical expression that defines a RSRQ threshold, and through this threshold it is possible to obtain a statistical classifier that detect if nodes are affected by collisions. Also, the CQI reports have been studied, the simulations have shown that exist a correlation between the percentage of TCQI with the COT of the interferer cell, which can be useful to have an idea about the channel status over UE located in border cells. The results show that the TCQI as well the RSRQ threshold can be used as predictive methods to detect if UEs are affected by collision in scenarios where eNBs are in hidden conditions.

We have developed an algorithm based on both metrics. This algorithm has been tested under a simulation campaign where conditions such as lognormal and multipath losses, mobility of UE, different kinds of traffic and number of UEha have been considered. The outcomes show that the algorithm detects the number of collisions correctly in average the 95% of time when the marSinr = 0dB.

This work fulfills their initial objectives because a solution of low complexity, which uses a set of metrics such as RSRP, RSRQ and CQI and transmission procedures that are already well defined in the standard and are always present in any LTE device, has been obtained. Additionally, the algorithm is based on basic math operations and threshold comparisons, where the computational load is extremely reduced.

Certainly, there are some algorithms used as statistical classifiers that can be used for hidden node detection, such as KNN, SVM or Logistic Regression, etc. whose analyses are being considered for future research. However, the main advantage of our algorithm is that it offers good results with a low complexity and without necessity of training.

The obtained algorithm identifies UEs located in a hidden zone, whose services are affected by interferences. The issue of how and when to take the decision of changing the operation band from unlicensed to licensed band is a secondary interesting research topic that can be addressed in the future.

Lastly, LAA systems are considered to work as an extension of the spectrum, where the services that demand high QoS are performed in the licensed band, meanwhile the less demanding ones are executed in the unlicensed band. Nevertheless, it is true that in zones where the free spectrum is rarely used, it would be possible to locate high priority services. The analysis of these services and their limitations regarding to guaranteed QoS would be an interesting research topic for the future.

Acknowledgments

This work has been supported in part by the MICINN/FEDER under the projects RTI2018-095684-B-I00 and RTI2018-099063-B-I00, by the Government of Aragon (Reference Group T31_20R) and Iberoamerican Mobility Grant financed by Banco Santander - Universidad de Zaragoza.

Supplementary materials

Supplementary material associated with this article can be found, in the online version, at doi:10.1016/j.comnet.2020.107280.

References

[1] P. Jonsson, S. Carson, A. Torres, K.Ö. Per Lindberg, A. Karapantelakis, Ericsson Mobility Report (June 2019), (2019) 28.
[2] E. Pateromichelakis, O. Bulakci, C. Peng, J. Zhang, Y. Xia, LAA as a Key Enabler in Slice-Aware 5G RAN: challenges and opportunities, IEEE Commun. Stand. Mag 2 (2018) 29–35, doi:10.1109/mcomstd.2018.1700061.
[3] 3GPP-TR36.889, Study on licensed-assisted access to unlicensed spectrum, 2015.
[4] 3GPP, TS 36.211 V13.4.0 Technical specification group radio access network; Evolved Universal Terrestrial Radio Access (E-UTRA); Physical channels and modulation (Release 13), (2016) 171.
[5] A.M. Baswade, V. Sathya, B.R. Tamma, A.A. Franklin, Unlicensed carrier selection and user offloading in dense LTE-U networks, 2016, IEEE Globecom Work (2016), doi:10.1109/GLOCOMW.2016.7849071.
[6] 3GPP R1-145128, Avoiding hidden node problem by full-duplex radio from UE perspective, Inst. Inf. Ind. RAN1#79. (2014) 3.
[7] 3GPP R1-151047, Discussion on hidden node issue for LAA, Samsung, RAN1 Ad-Hoc Meet. (2015).
[8] M. Abusubaih, B. Rathke, A. Wolisz, A framework for interference mitigation in multi-BSS 802.11 wireless LANs, 2009 Proceedings of the IEEE International Symposium a World Wireless, Mob. Multimed. Networks Work. WOWMOM. (2009). 10.1109/WOWMOM.2009.5282490.
[9] S. Ray, D. Starobinski, On false blocking in RTS/CTS-based multihop wireless networks, IEEE Trans. Veh. Technol. 56 (2007) 849–862, doi:10.1109/TVT.2007.891476.
[10] , Discussion on hidden node problem for LAA, Huawei, HiSilicon, in: Proceedings of the RAN1 Ad-Hoc Meeting, 2015 March.
[11] 3GPP R2-154303, RSSI measurement for hidden node detection, 3GPP TSG RAN WG2, Malmö, Sweden, Oct. 5th – 9th. (2015).
[12] S. Han, Y.C. Liang, Q. Chen, B.H. Soong, Licensed-Assisted access for LTE in unlicensed spectrum: a MAC protocol design, IEEE J. Sel. Areas Commun. 34 (2016) 2550–2561, doi:10.1109/JSAC.2016.2605959.
[13] 3GPP, TS 136 300 - V10.11.0 - LTE; Evolved Universal Terrestrial Radio Access (E-UTRA) and Evolved Universal Terrestrial Radio Access Network (E-UTRAN); Overall description; Stage 2 (3GPP TS 36.300 version 10.11.0 Release 10), 10.11.0 (2013) 1–210.
[14] R. Zhang, M. Wang, L.X. Cai, Z. Zheng, X.S. Shen, L.L. Xie, LTE-unlicensed: the future of spectrum aggregation for cellular networks, IEEE Wirel. Commun. 22 (2015) 150–159, doi:10.1109/MWC.2015.7143339.
[15] B. Chen, J. Chen, Y. Gao, J. Zhang, Coexistence of LTE-LAA and Wi-Fi on 5 GHz with corresponding deployment scenarios: a survey, IEEE Commun. Surv. Tutor. 19 (2017) 7–32, doi:10.1109/COMST.2016.2593666.
[16] H.J. Kwon, J. Jeon, A. Bhorkar, Q. Ye, H. Harada, Y. Jiang, L. Liu, S. Nagata, B.L. Ng, T. Novlan, J. Oh, W. Yi, Licensed-assisted access to unlicensed spectrum in LTE Release 13, IEEE Commun. Mag. 55 (2017) 201–207, doi:10.1109/MCOM.2016.1500698CM.
[17] ETSI TS 136 213, Physical layer procedures (3GPP TS 36.213 version 13.0.0 Release 13), (2016) 328. http://www.etsi.org/standards-search (accessed March 3, 2018).
[18] B. Bojovic, L. Giupponi, Z. Ali, M. Miozzo, Evaluating Unlicensed LTE Technologies: LAA vs LTE-U, IEEE Access 7 (2019) 89714–89751, doi:10.1109/access.2019.2926197.
[19] ITU-R, Guidelines for evaluation of radio interface technologies for IMT-Advanced, International Telecommunication Union, Tech. Rep. ITU-R, M.2135-1. (2009) 72. https://www.itu.int/dms_pub/itu-r/opb/rep/R-REP-M.2135-1-2009-PDF-E.pdf (accessed January 23, 2018).
[20] ETSI, TS 36.104 V12.6.0 - LTE; Evolved Universal Terrestrial Radio Access (E-UTRA); Base Station (BS) radio transmission and reception (3GPP TS 36.104 version 12.6.0

Release 12), 2015. http://portal.etsi.org/chaircor/ETSI_support.asp (accessed December 28, 2018).
[21] C.-D. Iskander, A MATLAB-based object-oriented approach to multipath fading channel simulation, Ww2.Mathworks.Cn. (2008). http://ww2.mathworks.cn/matlabcentral/mlc-downloads/downloads/submissions/18869/versions/1/download/pdf/ChannelModelingWhitePaper.pdf (accessed January 1, 2019).
[22] 3GPP TR 36.814 V9.0.0, Evolved Universal Terrestrial Radio Access (E-UTRA); Further advancements for E-UTRA physical layer aspects (Release 9), 2010. ts_136211v090100p.
[23] P. Campos, A. Hernández-Solana, A. Valdovinos-Bardaji, Detection and impact of the hidden node problem in LAA-wifi coexistence scenarios, 2018, in: Proceedings of the 14th International Wireless Communications Mobile Computing Conference IWCMC 2018, 2018, pp. 1391–1397, doi:10.1109/IWCMC.2018.8450486.
[24] P. Campos, A. Hernández-Solana, A. Valdovinos-Bardají, Dealing with the hidden node problem in multioperator LAA-LTE scenarios, 2018 Proceedings of the IFIP/IEEE International Conference on Performance Evaluation and Modeling in Wired and Wireless Networks. (2018) 1–7. 10.23919/PEMWN.2018.8548936.
[25] N. et al. Baldo, Design Documentation, (2015). https://www.nsnam.org/docs/models/html/lte-design.html.
[26] ETSI, TS 136 133 - V14.3.0 - LTE; Evolved Universal Terrestrial Radio Access (E-UTRA); Requirements for support of radio resource management (3GPP TS 36.133 version 14.3.0 Release 14), 2017. https://portal.etsi.org/TB/ETSIDeliverableStatus.aspx (accessed December 20, 2018).
[27] ETSI, TS 136 331 - V14.2.2 - LTE; Evolved Universal Terrestrial Radio Access (E-UTRA); Radio Resource Control (RRC); Protocol specification (3GPP TS 36.331 version 14.2.2 Release 14), 2017. https://portal.etsi.org/TB/ETSIDeliverableStatus.aspx (accessed December 20, 2018).
[28] 3 GPP R1-152992, “CSI measurement and report for LAA”, TSG RAN WG1 Meeting #81, Fukuoka, Japan, 25th – 29th May, (2015) 4.
[29] 3 GPP R1-152868, “Discussion on CSI measurement and reporting for LAA”, TSG RAN WG1 Meeting #81 Fukuoka, Japan, 25th – 29th May, (2015).
[30] T.T.T. Nguyen, G. Armitage, P. Branch, S. Zander, Timely and continuous machine-learning-based classification for interactive IP traffic, IEEE/ACM Trans. Netw. 20 (2012) 1880–1894, doi:10.1109/tnet.2012.2187305.

Pablo Campos obtained the Engineer of Telecommunications degree from the Polytechnic National School (EPN), Ecuador, in 2004 and his Master degree from Polytechnic University of Turin in 2006 in Wireless Systems and Related Technologies. He is pursuing his PhD in Information Technologies and Communications in Mobile Networks at University of Zaragoza. His research interest includes 5G/4G technologies, heterogeneous networks with emphasis on radio resource management, quality of service and machine learning.

Ángela Hernández Solana obtained the Engineer of Telecommunications and Ph.D. degrees from the Universitat Politècnica de Catalunya (UPC), Spain, in 1997 and 2005, respectively. She has been working at UPC and at UNIZAR, where she is an Associate Professor since 2010. She is member of the Aragón Institute of Engineering Research (I3A). Her research interests include 5G/4G technologies, heterogeneous communication networks and mission-critical communication networks, with emphasis on transmission techniques, radio resource management and quality of service, mobility management and planning and dimensioning of mobile networks.

Antonio Valdovinos Bardají obtained the Engineer of Telecommunications and Ph.D. degrees from the Universitat Politècnica de Catalunya (UPC), Spain, in 1990 and 1994, respectively. He has been working at UPC and at the University of Zaragoza (UZ), where he is a Full Professor since 2003. His research interests include 5G/4G technologies, heterogeneous communication networks and mission-critical communication networks, with emphasis on transmission techniques, radio resource management and quality of service, mobility management and planning and dimensioning of mobile networks.